PLOS ONE

RESEARCH ARTICLE

Oxylipin biosynthetic gene families of *Cannabis sativa*

Eli J. Borrego[1]*, Mariah Robertson[1], James Taylor[2], Zachary Schultzhaus[3], Elida M. Espinoza[4]

1 Rochester Institute of Technology, Thomas H. Gosnell School of Life Sciences, Rochester, NY, United States of America, **2** Department of Plant Pathology and Microbiology, Texas A&M University, College Station, TX, United States of America, **3** Independent Researcher, Fort Washington, MD, United States of America, **4** EnviroFlight, Apex, NC, United States of America

* eli.borrego@gmail.com

Check for updates

OPEN ACCESS

Citation: Borrego EJ, Robertson M, Taylor J, Schultzhaus Z, Espinoza EM (2023) Oxylipin biosynthetic gene families of *Cannabis sativa*. PLoS ONE 18(4): e0272893. https://doi.org/10.1371/journal.pone.0272893

Editor: Humberto Julio Debat, National Institute of Agricultural Technology (INTA), ARGENTINA

Received: July 27, 2022

Accepted: March 16, 2023

Published: April 26, 2023

Copyright: © 2023 Borrego et al. This is an open access article distributed under the terms of the Creative Commons Attribution License, which permits unrestricted use, distribution, and reproduction in any medium, provided the original author and source are credited.

Data Availability Statement: All relevant data are within the paper and its Supporting Information files.

Funding: The authors would like to acknowledge the generous support provided by the Thomas H. Gosnell School of Life Sciences (GSoLS) and the College of Science (COS) at the Rochester Institute of Technology (RIT). The funders had no role in study design, data collection and analysis, decision to publish, or preparation of the manuscript.

Competing interests: The authors have declared that no competing interests exist.

Abstract

Cannabis sativa is a global multi-billion-dollar cash crop with numerous industrial uses, including in medicine and recreation where its value is largely owed to the production of pharmacological and psychoactive metabolites known as cannabinoids. Often underappreciated in this role, the lipoxygenase (LOX)-derived green leaf volatiles (GLVs), also known as the scent of cut grass, are the hypothetical origin of hexanoic acid, the initial substrate for cannabinoid biosynthesis. The LOX pathway is best known as the primary source of plant oxylipins, molecules analogous to the eicosanoids from mammalian systems. These molecules are a group of chemically and functionally diverse fatty acid-derived signals that govern nearly all biological processes including plant defense and development. The interaction between oxylipin and cannabinoid biosynthetic pathways remains to be explored. Despite their unique importance in this crop, there has not been a comprehensive investigation focusing on the genes responsible for oxylipin biosynthesis in any *Cannabis* species. This study documents the first genome-wide catalogue of the *Cannabis sativa* oxylipin biosynthetic genes and identified 21 *LOX*, five allene oxide synthases (*AOS*), three allene oxide cyclases (AOC), one hydroperoxide lyase (*HPL*), and five 12-oxo-phytodienoic acid reductases (*OPR*). Gene collinearity analysis found chromosomal regions containing several isoforms maintained across *Cannabis*, *Arabidopsis*, and tomato. Promoter, expression, weighted co-expression genetic network, and functional enrichment analysis provide evidence of tissue- and cultivar-specific transcription and roles for distinct isoforms in oxylipin and cannabinoid biosynthesis. This knowledge facilitates future targeted approaches towards *Cannabis* crop improvement and for the manipulation of cannabinoid metabolism.

Introduction

For millennia, the diploid dioecious shrub *Cannabis sativa*, has been cultivated for its fiber, grain, and pharmacological properties [1]. Originating in Asia and now grown globally [2], *C. sativa* is a multibillion-dollar cash crop [3, 4] with many uses [5] including feed [6], textile [7],

biofuel [8], medicine [9], and recreation [10, 11]. The latter two of which are due to the production of biologically active metabolites, known as cannabinoids, within the cannabis trichomes [12]. Cannabinoids are a large chemical family with 130 currently known distinct chemical species [13] grouped into 10 structural types [14]. Undeniably, the best understood are the cannabidiol (CBD) [15] and psychoactive Δ^9-tetrahydrocannabinol (THC) [16]. Given their growing therapeutic uses and social acceptance, efforts are underway to produce chemotypes with explicit cannabinoid content [17, 18], platforms for heterologous production [19], and novel cannabinoid analogues [20].

The understanding of cannabinoid biosynthesis has made strides in recent years [12, 19, 21]. Briefly, cannabinoids are synthesized from the convergence of a fatty acid and terpene pathway. Hexanoic acid is activated into hexanoyl-CoA by acyl-activating enzyme 1 and subsequently elongated with three molecules of malonyl-CoA by TETRAKETIDE SYNTHASE (TSK, also known as OLIVETOL SYNTHASE). TKS functions in concert with OLIVETOLIC ACID CYCLASE to generate olivetolic acid. Geranyl pyrophosphate produced from the non-mevalonate-dependent isoprenoid pathway (MEP) is used by CANNABIGEROLIC ACID SYNTHASE to prenylate olivetolic acid into cannabigerolic acid (CBGA), the first *bona fide* cannabinoid. CBGA can then be shunted into one of at least three oxidocyclization sub-branches to produce tetrahydrocannabinolic acid (THCA), cannabidiolic acid (CBDA), and cannabichromenic acid (CBCA) by THCA SYNTHASE, CBDA-SYNTHASE, and CBCA SYNTHASE, respectively. Later, THCA, CBDA, CBCA may undergo nonenzymatic decarboxylation into the better-known THC, CBD, or cannabichromene (CBC). Lastly, cannabinoids may also undergo spontaneous rearrangements that are responsible for the structural variation found within this chemical family [12, 13, 22].

Despite the recent advances in the understanding of the cannabinoid biosynthetic pathway, the origin of hexanoic acid (also known as caproic acid) remains unclear. It is often the rate-limiting step in heterogenous systems [20, 23] requiring hexanoic acid as a feedstock [19]. In *planta*, trichome-specific transcriptomic analysis observed co-expression of genes involved in oxylipin biosynthesis, namely *LIPOXYGENASE* (*LOX*) and *HYDROPEROXIDE LYASE* (*HPL*), with genes previously established in cannabinoid biosynthesis [24, 25]. This has prompted the hypothesis that the oxylipin pathway provides the substrate required for cannabinoid biosynthesis. Further, this putative oxylipin-cannabinoid interaction invites exploration to understand the role of the oxylipins in cannabinoid biosynthesis and *Cannabis* biology.

Oxylipins are a large group of oxidized fatty acid-derivatives possessing potent signaling activities that govern a multitude of physiological processes including, growth, development, and defense [26]. In plants, the majority of oxylipin biosynthesis occurs via the LOX pathway. It begins with the regio- and stereo-specific incorporation of molecular oxygen at either the 9^{th}—or 13^{th} -carbon of linoleic (C18:2) or linolenic (C18:3) acid by 9- or 13-LOX isoforms [27]. The resulting 9- or 13-oxylipins can be fluxed into at least one of seven sub-branches to produce chemically diverse groups of distinct chemical species, including alcohols, aldehydes, divinyl ethers, esters, epoxides, hydroxides, hydroperoxides, ketols, ketones, and triols. Though the biological role for the vast majority of plant oxylipins remains to be deciphered, investigations of selected members of 13-oxylipins, namely jasmonates and green leaf volatiles (GLVs) have spearheaded a framework towards understanding their physiological and ecological roles.

Jasmonates are best known for their roles in providing defense against insects and necrotrophic pathogens [28]. Jasmonates are cyclopentones produced through the ALLENE OXIDE SYNTHASE (AOS) subbranch [29, 30]. Following the oxygenation of C18:3 to 13[*S*]-hydroperoxyoctadecatrienoic acid (13-HPOT) by 13-LOX activity, AOS [29, 31, 32] converts 13-HPOT to 12,13(*S*)-epoxy-octadecatrienoic acid (12,13-EOT) and ALLENE OXIDE

CYCLASE (AOC) [33] converts 12,13-EOT to (+)-*cis*-12-oxo-phytodienoic acid (12-OPDA), the first jasmonate in the pathway. LOX, AOS, and AOC are closely associated with each other and participate in substrate channeling during jasmonate biosynthesis [34]. Aside from serving as a substrate for downstream reactions, 12-OPDA possesses its own distinct activity [35–37]. 12-OPDA is reduced via 12-OXO-PHYTODIENOIC ACID REDUCTASE (OPR) [38, 39] to 9*S*,13*S*-OPDA to 3-oxo-2-(2′[*Z*]-pentenyl)-cyclopentane-1-octanoic acid (OPC-8:0) and then undergoes three rounds of β-oxidations to produce (+)-7-iso-jasmonic acid (JA) [40]. Hexadecatrienoic acid (C16:3) may also serve as a substrate for jasmonate biosynthesis, eliminating the need for a round of β-oxidation [41–43]. While a multitude of JA derivates have been identified [29], (+)-7-iso-jasmonoyl-L-isoleucine (JA-Ile) is the best studied, owed to its service as a ligand in receptor-mediated perception and subsequent signaling [44].

GLVs are best known as the scent of cut grass and are involved in defense signaling, plant-to-plant and plant-to-insect communication [45]. They are C_6 volatile aldehydes, alcohols, and their acetyl esters produced through the HPL subbranch [46, 47]. Here, the 13-hydroperoxy fatty acids produced from 13-LOX activity from either C18:2 or C18:3 are cleaved, respectively, by 13-HPL [48–50] into the hexanal or (3*Z*)-hexenal and 12-oxo-(9*Z*)-dodecenoic acid. The latter of which is the progenitor of the traumatin sub-group, of which some members display signaling activity independent of GLVs [51]. Additionally, C16:3 may also serve as a fatty acid substrate for GLV biosynthesis, yielding (7*Z*)-10-oxo-decenoic acid in place of traumatin [52]. The GLV aldehydes are reduced to alcohols through reductase [53] and acetylated through acetyltransferase [54]. Finally, (3Z)-hexenal can also be isomerized through (3Z):(2E)-ENAL ISOMERASE [55, 56].

Thus, this study sought to elucidate the *Cannabis* oxylipin biosynthetic pathway as a source for cannabinoid substrate and molecular signals important in defense and development. Here, a census was conducted on the *C*. *sativa* genome to catalog the major oxylipin biosynthetic genes from the LOX, AOS, AOC, and OPR gene families. Respectively, their chromosomal locations, conserved protein domains, genetic structures, and phylogenetic relationships were determined. Collinearity analysis identified several genes in syntenic regions with *Arabidopsis* and tomato. The promoter analysis revealed evidence for tissue- and stimulus-specific transcriptional regulation, which stands in agreement with expression observed from a *Cannabis* transcriptome atlas and publicly-available transcriptomes. Finally, gene co-expressional network and functional enrichment analysis identified genetic modules that implicate oxylipin biosynthetic genes in distinct *Cannabis* physiological processes.

Materials and methods

Gene model identification, protein domain analysis, and subcellular localization prediction

The *Cannabis sativa* representative genome cs10 [57] was surveyed for LOX, AOS, HPL, AOC, and OPR gene models using the NCBI BLASTP algorithm against the *Arabidopsis* sequences as the input queries. The corresponding public transcriptome data was explored through the NCBI Genome Data Viewer [58] to obtain gene models and evidence of transcription and putative translation. Amino acid sequences were examined against the NCBI Conserved Domain Database for the presence of canonical domains using Batch CD-Search [59, 60]. Conserved peptide sequence motifs were determined using MEME 5.4.1 [61, 62] for up to 25 motifs and any number of repetitions. Subcellular localization prediction analysis was performed using DeepLoc 1.0 [63], LOCALIZER [64], Plant-mSubP [65], and TargetP 2.0 [66] through their web servers with default settings.

Multiple sequence alignment, phylogenetic analysis, and genetic structure visualization

Peptide sequences were aligned through the online version of MAFFT [67, 68] using the FFT-NS-I iterative refinement strategy, leaving gappy regions, and with other settings as default. Phylogenetic trees were generated through the MAFFT website using neighbor-joining, Jones-Taylor-Thornton substitution model, with estimated heterogeneity. Trees were tested with bootstrapping of 1000 resampling and drawn with FigTree 1.4.1. Gene structures were visualized with TBtools v1.098689 [69] using the NCBI *Cannabis sativa* Annotation Release 100.

Promoter analysis of cis-regulatory elements

Putative cis-acting regulatory elements were determined using the 1.5 kb upstream nucleotide sequences of gene models, analyzed with PlantCARE [70], and promoter diagrams were constructed with TBtools.

Comparative genomic analysis

Gene collinearity between *C. sativa-Arabidopsis thaliana* (reference genome TAIR10.1) and *C. sativa-Solanum lycopersicum* (representative genome SL3.0) was performed using MCScanX [71] feature of TBtools with an e-value 1e-10 and 5 BLAST hit cutoffs.

Transcriptomic profiling, regulatory network analysis

RNA-Seq SRP achieved data was retrieved from GEO Datasets, SRP234963 [72] and SRP168446 [73], and trimmed with fastp v0.23.1 [74] using default settings. Transcripts Per Million (TPM) were calculated using salmon [75] mapping-based mode against a decoy-aware transcriptome file. Corrections were made for fragment-level GC content and random hexamer primer biases. Transcriptome indices were computed from the cs10 reference transcriptome against its respective genome.

Gene co-expression networks were generated through an iterative weighted correlation network analysis (WGCNA) using iterativeWGCNA with default parameters [76, 77]. Relationships between highly interconnected gene modules were explored through an eigengene score correlation matrix visualized through Cytoscape [78].

Functional enrichment analysis was performed with g:Profiler [79] using orthologues identified through PLAZA 5.0 [80] and cross-referenced against the Kyoto Encyclopedia of Genes and Genomes [81–83] and Gene Ontology Database [84, 85].

Results

Cannabis oxylipin biosynthetic genes

To establish a foundation for *Cannabis* oxylipin biology, the *C. sativa* oxylipin biosynthetic genes were determined. The *C. sativa* representative genome was queried against selected *Arabidopsis* LOX, AOS, HPL, AOC, and OPR amino acid [19] sequences with BLASTP to detect candidate *C. sativa* orthologues. The analysis identified 21 LOX, six CYP74, three AOC, and five OPR gene models. Moreover, each was predicted to encode proteins that were functionally annotated within NCBI as members of these groups of oxylipin biosynthetic genes (Table 1).

The genes were found asymmetrically distributed both across and within the 10 *C. sativa* chromosomes (Fig 1) with the largest concentration of genes found on Chromosome 1, 2, and 9. Over 60% of the LOX isoforms were found on Chromosome 2, and with the exception of

Table 1. Genes encoding LOX, CYP74, AOC, and OPR isoforms of *C. sativa* and their predicted peptide subcellular localization.

Annotation	NCBI Annotation	Locus	Chromosome	Location	Sense	mRNA	Protein	AA		DeepLOC	LOCALIZER	mSubP	TargetP
CsLOX1	probable linoleate 9S-lipoxygenase 5	LOC115719608	2	48717953..48726423	-	XM_030648706.1	XP_030504566	860		Cytoplasm	-	Cyto	-
CsLOX2	probable linoleate 9S-lipoxygenase 5	LOC115718693	2	48399032..48404403	-	XM_030647516.1	XP_030503376	955		Plastid	-	Plastid	-
CsLOX3	probable linoleate 9S-lipoxygenase 5	LOC115724062	9	45035547..45040076	-	XM_030653517.1	XP_030509377	872		Cytoplasm	-	Cyto	-
CsLOX4	probable linoleate 9S-lipoxygenase 5	LOC115709296	3	1987993..1993483	+	XM_030637370.1	XP_030493230	859		Cytoplasm	-	Cyto	-
CsLOX5	probable linoleate 9S-lipoxygenase 5	LOC115720291	2	48437789..48443653	-	XM_030649445.1	XP_030505305	848		Cytoplasm	-	Cyto	-
CsLOX6	probable linoleate 9S-lipoxygenase 5 Isoform X1	LOC115721132	2	48616833..48624053	-	XM_030650384.1	XP_030506244	859		Cytoplasm	-	Cyto	-
CsLOX7	probable linoleate 9S-lipoxygenase 5	LOC115719336	2	48633009..48641095	-	XM_030648324.1	XP_030504184	871		Cytoplasm	-	Cyto	-
CsLOX8	probable linoleate 9S-lipoxygenase 5	LOC115722276	9	58835655..58849094	+	XM_030651442.1	XP_030507302	868		Cytoplasm	-	Cyto	-
CsLOX9	linolate 9S-lipoxygenase 6	LOC115721268	2	3929913..3935080	+	XM_030650533.1	XP_030506393	875		Cytoplasm	-	Cyto	-
CsLOX10	probable linoleate 9S-lipoxygenase 5	LOC115722275	9	58804514..58809886	+	XM_030651441.1	XP_030507301	868		Cytoplasm	-	Cyto	-
CsLOX11	probable linoleate 9S-lipoxygenase 5	LOC115723988	9	58775266..58790926	+	XM_030653445.1	XP_030509305	873		Cytoplasm	-	Cyto	-
CsLOX12	linoleate 9S-lipoxygenase 1	LOC115718785	2	181580..185609	-	XM_030647611.1	XP_030503471	838		Mitochondrion	Mitochondrion	Endoplasm	mTP
CsLOX13	lipoxygenase 6, chloroplastic isoform X1	LOC115712696	4	8039511..8043316	+	XM_030641024.1	XP_030496884	935		Plastid	cTP	Plastid	cTP
CsLOX14	linoleate 13S-lipoxygenase 3–1, chloroplastic	LOC115707105	1	89971772..89976562	-	XM_030634953.1	XP_030490813	931		Plastid	cTP	Plastid	-
CsLOX15	linoleate 13S-lipoxygenase 2–1, chloroplastic isoform X1	LOC115719612	2	93914675..93922215	+	XM_030648714.1	XP_030504574	929		Plastid	cTP	Cyto	-
CsLOX16	linoleate 13S-lipoxygenase 2–1, chloroplastic	LOC115719614	2	93928923..93935412	+	XM_030648717.1	XP_030504577	926		Plastid	-	Cyto	-
CsLOX17	linoleate 13S-lipoxygenase 2–1, chloroplastic	LOC115720530	2	93947032..93955004	+	XM_030649675.1	XP_030505535	1293		Plastid	-	Plastid	-
CsLOX18	linoleate 13S-lipoxygenase 2–1, chloroplastic	LOC115719613	2	93802540..93809737	+	XM_030648716.1	XP_030504576	929		Plastid	cTP	Plastid	cTP
CsLOX19	linoleate 13S-lipoxygenase 2–1, chloroplastic	LOC115719615	2	93892217..93901839	+	XM_030648718.1	XP_030504578	922		Plastid	cTP	Plastid	-
CsLOX20	linoleate 13S-lipoxygenase 2–1, chloroplastic	LOC115719616	2	93836391..93848870	+	XM_030648719.1	XP_030504579	917		Plastid	-	Plastid	-
CsLOX21	linoleate 13S-lipoxygenase 2–1, chloroplastic	LOC115719617	2	93822415..93829745	+	XM_030648721.1	XP_030504581	909		Plastid	cTP	Plastid	-
CsAOS1	allene oxide synthase 1, chloroplastic-like	LOC115723125	9	2271373..2273482	+	XM_030652553.1	XP_030508413	525		Plastid	cTP	Plastid	cTP
CsAOS2	allene oxide synthase 3	LOC115703182	X	6627388..6629208	+	XM_030630703.1	XP_030486563	482		Peroxisome	-	Celmemb	-
CsAOS3	allene oxide synthase 3	LOC115708244	1	22613465..22615178	+	XM_030636464.1	XP_030492324	483		Plastid	-	Celmemb	-
CsAOS4	allene oxide synthase 3	LOC115722144	9	55962020..55963631	+	XM_030651275.1	XP_030507135	503		Plastid	-	Celmemb	-
CsAOS5	allene oxide synthase 3	LOC115703186	X	6682344..6684188	-	XM_030630707.1	XP_030486567	503		Plastid	-	Celmemb	-
CsHPL	fatty acid hydroperoxide lyase, chloroplastic	LOC115698766	8	51951025..51958560	+	XM_030625939.1	XP_030481799	485		Plastid	-	Plastid	-

(*Continued*)

Table 1. (Continued)

Annotation	NCBI Annotation	Locus	Chromosome	Location	Sense	mRNA	Protein	AA		DeepLOC	LOCALIZER	mSubP	TargetP
CsAOC1	allene oxide cyclase, chloroplastic	LOC115701324	8	54784220..54785234	+	XM_030629083.1	XP_030484943	183		Cytoplasm	-	Celmemb	-
CsAOC2	allene oxide cyclase, chloroplastic	LOC115700991	8	54774852..54776132	-	XM_030628671.1	XP_030484531	249		Plastid	cTP	Plastid	cTP
CsAOC3	allene oxide cyclase, chloroplastic	LOC115699327	8	35236892..35238108	+	XM_030626678.1	XP_030482538	257		Plastid	cTP	Plastid	cTP
CsOPR1	12-oxophytodienoate reductase 3 isoform X1	LOC115706391	1	27999501..28002834	-	XM_030634031.1	XP_030489891	452		Peroxisome	cTP	Plastid	-
CsOPR2	LOW QUALITY PROTEIN: 12-oxophytodienoate reductase 3-like	LOC115706393	1	27991920..27994962	-	XM_030634033.1	XP_030489893	392		Peroxisome	-	-	-
CsOPR3	12-oxophytodienoate reductase 3-like	LOC115706394	1	27977420..27994954	-	XM_030634034.1	XP_030489894	392		Peroxisome	-	Cyto	-
CsOPR4	12-oxophytodienoate reductase 3-like	LOC115703964	1	27889405..27891439	-	XM_030631189.1	XP_030487049	392		Peroxisome	-	Cyto	-
CsOPR5	putative 12-oxophytodienoate reductase 11	LOC115722904	9	35363370..35365841	-	XM_030652270.1	XP_030508130	371		Peroxisome	cTP	Cyto	cTP

https://doi.org/10.1371/journal.pone.0272893.t001

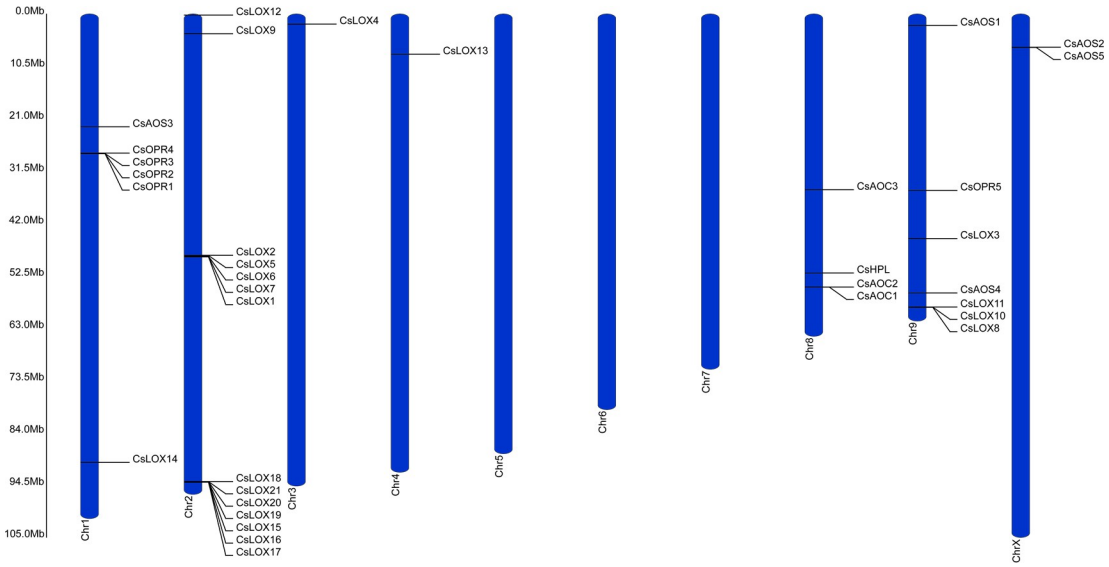

Fig 1. Distribution of the LOX, AOS, HPL, AOC, and OPR gene families across the *C. sativa* genome. Ruler depicts chromosome length.

https://doi.org/10.1371/journal.pone.0272893.g001

two, were in large gene clusters. *CsLOX1*, *2*, *5*, *6*, and *7* were located in a 327 kb region in the center of Chromosome 2, while *CsLOX15*, *16*, *17*, *18*, *19*, *20*, and *21* were near the outer arm in a 152 kb region (S1 Fig). A smaller 74 kb region on Chromosome 9 contained the cluster of *CsLOX8*, *10*, and *11* towards the end of a chromosomal arm. *CsLOX9* and *12* were relatively close together on Chromosome 2, while Chromosomes 1, 3, and 4 contained single LOX isoforms, *CsLOX14*, *4*, and *13*, respectively.

Similar to the *LOX* genes, members of the CYP74, AOC, and OPR gene families were found in gene clusters at nearly the same proportions. On Chromosome 8, CsAOS2 and 5 were within 57 kb from each other (S2 Fig). The other *CYP74* genes, *CsAOS1*, *CsHPL*, *CsAOS1*, and *CsAOS4* were on Chromosomes 1, 8, and 9, respectively. *AOC* genes were found exclusively on Chromosome X with *CsAOC1* and *2* only 10 kb apart (S2 Fig). Strikingly, with the exception of *CsOPR5* located on Chromosome 9, the entire OPR gene family was confined to a 113 kb segment on Chromosome 1.

The C. sativa LOX gene family contains 21 members

To verify that candidate LOX gene models encode functional isoforms, their peptide sequences were examined for the presence of the lipid-associated PLAT and catalytic LOX domains archetypical of LOX proteins [27]. Amino acids were examined through the NCBI Conserved Domain Database function and all 21 gene models encoded peptides that displayed both domains, providing support that *C. sativa* possesses 21, *bona fide*, LOX isoforms (Fig 2A). Unexpectedly, the analysis revealed that *CsLOX17* also contained a RVT2 and a RNAse H-like domain which may indicate the insertion of a retrotransposon in its upstream region [86, 87].

Analysis of conserved motifs showed that the majority of the LOX isoforms contain similar composition and distribution of amino acid sequence patterns (Fig 2B). Nearly all isoforms displayed the same 13 motif arrangement, typical of LOX proteins, on the N-terminus, a highly conserved region which requires stringent composition for enzymatic activity. The exception was CsLOX12 which was absent of motif 13. Aside from CsLOX1 and 14, the arrangement of the first 5 motifs on the C-terminus was broadly consistent across all the proteins. However,

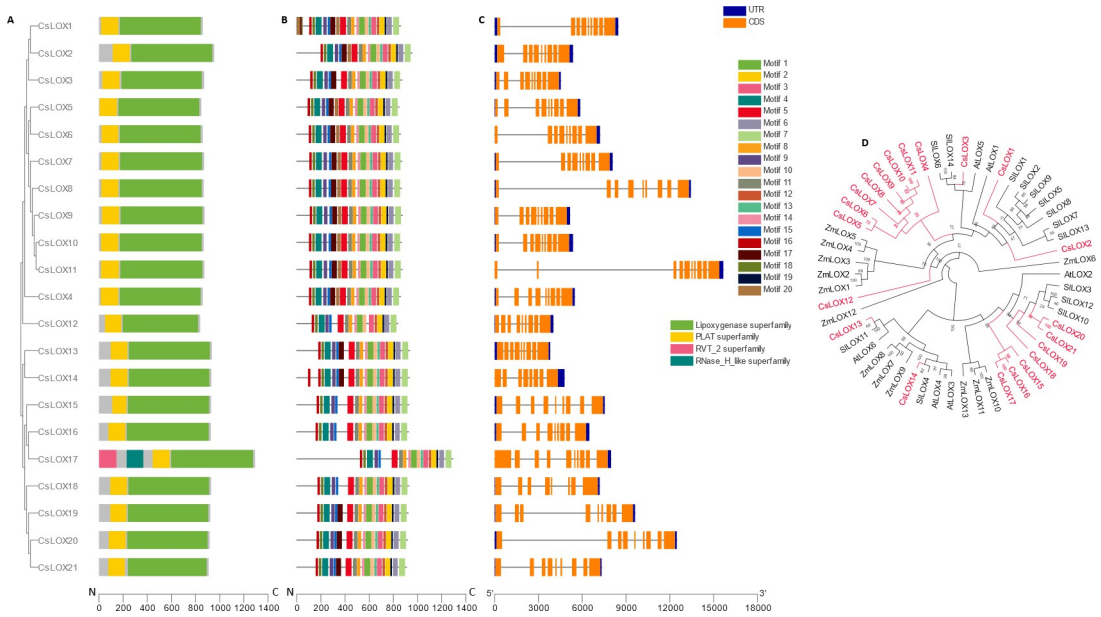

Fig 2. Phylogenetic, genetic, motif, and domain analysis of the CsLOX gene family. (A) Cladogram of peptide sequences and conserved domains. **(B)** Distribution of conserved peptide sequence motifs. Colors are described in legend; x-axis represents length of peptides in amino acids. **(C)** Diagram of genetic structure. Blue bars, orange bars, and gray lines represent untranslated regions, exons, and introns, respectively; x-axis represents length of gene in nucleotides. **(D)** Polar cladogram depicting evolutionary relationship with gene families of selected species. Node labels show confidence values from 1000 bootstrap replications.

https://doi.org/10.1371/journal.pone.0272893.g002

several isoforms possessed regions where no motifs were detected. In LOX proteins, these regions typically contain highly divergent, transient peptide sequences that direct subcellular localization [88]. In support of this notion, their amino acid sequences were tested against four subcellular prediction algorithms, DeepLOC, LOCALIZER, mSUBP, and TargetP (Table 1). A consensus of plastid localization was reached for only CsLOX13 and CsLOX18, along with an agreement of the majority of the software localizing CsLOX2, CsLOX14, CsLOX15, CsLOX17, CsLOX18, CsLOX19, CsLOX20, and CsLOX21 to this organelle. CsLOX1 and CsLOX3-11 were predicted to be found in the cytoplasm. Interestingly, CsLOX12 was predicted to be associated with the mitochondria.

Motifs 17 and 20 located within the LOX domain showed the largest variability across the LOX isoforms. The former was absent from CsLOX3, 13, and 14, the latter was missing from CsLOX19 and 20, and both were missing from CsLOX12, 15, 16, 17, and 18, prompting the speculation of divergent catalytic activity among even closely related members [89].

The *C. sativa* LOX gene models ranged in size from around 4 to 16 kb and over 75% possessed eight introns (Fig 2C). A recurrent observation in the genetic structures of some *LOX* family members was the presence of a large first or second intron, e.g., CsLOX1, 6, 7, 8, 11, and 20 comprising of about 50 to 60% of the entire gene. No data is yet available for alternative splicing or transcript variants of these genes to provide insight into the role of these features.

Plant LOXs are typically grouped as 9- or 13-LOXs according to their major enzymatic product and isoforms with similar activity display higher sequence similarity and evolutionary relationships [27]. To designate the classification of *C. sativa* LOXs, their peptide sequences were compared to dicot and monocot plant species with well-characterized LOX protein families, namely, *A. thaliana*, *C. sativa*, *S. lycopersicum*, *and Zea mays* (Fig 2D). CsLOX1, 2, and 3 grouped with the *Arabidopsis* 9-LOXs, AtLOX1 and 5, respectively. Remarkably, eight

Cannabis LOXs peptides, CsLOX4-11, formed a *Cannabis* specific clade nested within monocot and dicot 9-LOXs. CsLOX12 was difficult to place within the tree, a result which was likely related to the absence of the three variable peptide motifs in its catalytic domain (Fix. 2B). CsLOX13 and 14 clustered with clades containing dicot 13-LOXs. Interestingly, seven *Cannabis* LOX peptides, CsLOX15-21 grouped with the 13-LOX clade, and several of which may represent *Cannabis*-specific 13-LOXs. Thus, *C. sativa* possess eleven 9-LOXs (CsLOX1–11), nine 13-LOXs (CsLOX13–21), and one that remains to be empirically determined (CsLOX12).

The *C. sativa* CYP74 gene family contains six members

AOS and HPL belong to the atypical CYP74 clade of the P450 family involved in hydroperoxyl fatty acid rearrangement or dismutation [90]. Amino acid sequence analysis found a single CYP74 domain in all six *Cannabis* candidate CYP74s and four distinct patterns of conserved sequence motifs (Fig 3A and 3B). The pattern variations were most pronounced towards the N-termini where each possessed a distinctive starting motif. The N-terminus of CYP74s typically possess transient peptide signals involved in directing their subcellular localizations towards plastids, and while subsequent analysis prediction supported this notion in CsHPL and CsAOS1, a consensus among the four software prediction tools could not be reached for CsAOS2-5 (Table 1). For gene structure analysis, CsHPL was notable for the presence of two introns (Fig 3C), an unusual feature of CYP74 family members, one of which comprised the majority of its gene model sequence.

While many CYP74 isoforms display multifunctionality [91], catalyzing varying proportions of AOS, epoxy alcohol synthase (EAS), divinyl ether synthase (DES), and HPL products, the CYP74A and CYP74B clade members show predominantly AOS and HPL activities, respectively. To understand the potential function of *C. sativa* CYP74 family members, a phylogenetic analysis assessed their relationship within the relatively well-characterized CYP74 subclades from diverse plant species (Fig 3D). CsAOS1 and CsHPL were grouped within the CYP74A and CYP74B clades, respectively. However, the placement of CsAOS2-4 proved challenging. Nonetheless, CsAOS2 and 3 and CsAOS4 and 5 grouped as pairs roughly within CYP74C.

Taken together, this analysis suggests that *C. sativa* contains at least two dedicated CYP74 enzymes that, given their phylogenies and subcellular localization, are specialized for 13-AOS

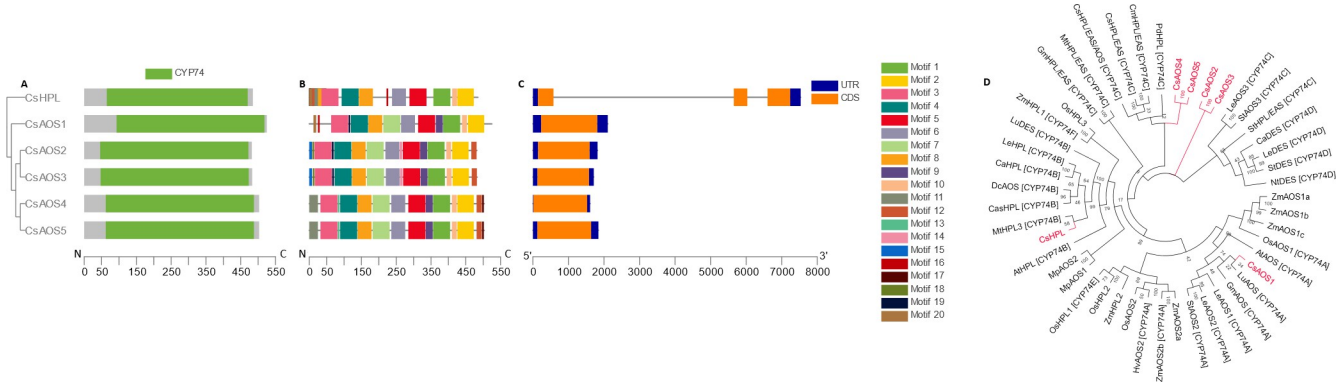

Fig 3. Phylogenetic, genetic, motif, and domain analysis of the *C. sativa* CYP74 gene family. (A) Cladogram of peptide sequences and conserved domains. **(B)** Distribution of conserved peptide sequence motifs. Colors are described in legend; x-axis represents length of peptides in amino acids. **(C)** Diagram of genetic structure. Blue bars, orange bars, and gray lines represent untranslated regions, exons, and introns, respectively; x-axis represents length of gene in nucleotides. **(D)** Polar cladogram depicting evolutionary relationship with gene families of selected species. Node labels show confidence values from 1000 bootstrap replications.

https://doi.org/10.1371/journal.pone.0272893.g003

and HPL activity, thus capable of providing substrate for JA or GLV biosynthesis. *Cannabis* also contains four CYP74 isoforms with unassigned activities.

The *C. sativa* AOC gene family contains three members

AOC provides steric hindrance for the stereospecific cyclization of allene oxide to 12-OPDA, the parent jasmonate species. All three CsAOC isoforms contain an AOC domain and similar amino acid sequence patterns on the last six motifs of their C-termini (Fig 4A and 4B). CsAOC2 and CsAOC3 displayed substantial variability in predicted motifs at their N-termini, likely corresponding to putative plastid transient peptide sequences (Table 1). CsAOC1 was predicted to localize outside of the plastids. The intron-exon distribution of this gene family differed mildly with CsAOC1 and 2 having three exons while CsAOC3 contained one (Fig 4C). To understand the evolutionary relationship of the *C. sativa* AOC gene family, their peptide sequences were analyzed phylogenetically with AOC members from other plant species [92]. CsAOC1 and 2 clustered close to each other within a dicot specific clade and CsAOC3 grouped into a separate dicot-specific clade that contained all *Arabidopsis* AOCs (Fig 4D).

The *C. sativa* OPR gene family contains five members

All five identified *C. sativa* OPR candidates were found to contain the conserved Old Yellow Enzyme-like domain necessary for their activity (Fig 5A) [93]. CsOPR1-4 had nearly identical patterns of amino acid sequence motifs and were largely similar to the motif arrangement of CsOPR5, however, the latter isoform lacked four conserved motifs (Fig 5B). In regard to their genetic structure, a substantial first intron was identified in CsOPR3, resulting in a gene model roughly three times larger than the other isoforms (Fig 5C). It is important to note that the current gene model of CsOPR3 appears chimeric with CsOPR2 in the current *C. sativa* representative genome (S2 Fig).

To investigate the evolutionary relationship between the *C. sativa* OPR gene family members, the amino acid sequences were compared to OPR family members from dicots and monocots. CsOPR1-4 formed a phylogenetic clade with the JA-producing AtOPR3. CsOPR5, however, was grouped with Type-II OPRs (Fig 5D). Taken together, *C. sativa* contains four Type-I OPR isoforms that are likely involved in classical JA biosynthesis.

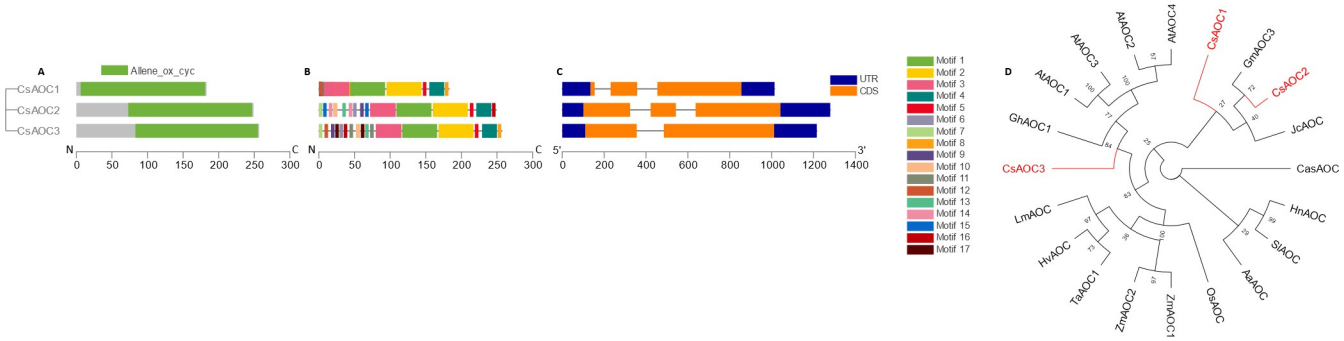

Fig 4. Phylogenetic, genetic, motif, and domain analysis of the CsAOC gene family. (A) Cladogram of peptide sequences and conserved domains. **(B)** Distribution of conserved peptide sequence motifs. Colors are described in legend; x-axis represents length of peptides in amino acids. **(C)** Diagram of genetic structure. Blue bars, orange bars, and gray lines represent untranslated regions, exons, and introns, respectively; x-axis represents length of gene in nucleotides. **(D)** Polar cladogram depicting evolutionary relationship with gene families of selected species. Node labels show confidence values from 1000 bootstrap replications.

https://doi.org/10.1371/journal.pone.0272893.g004

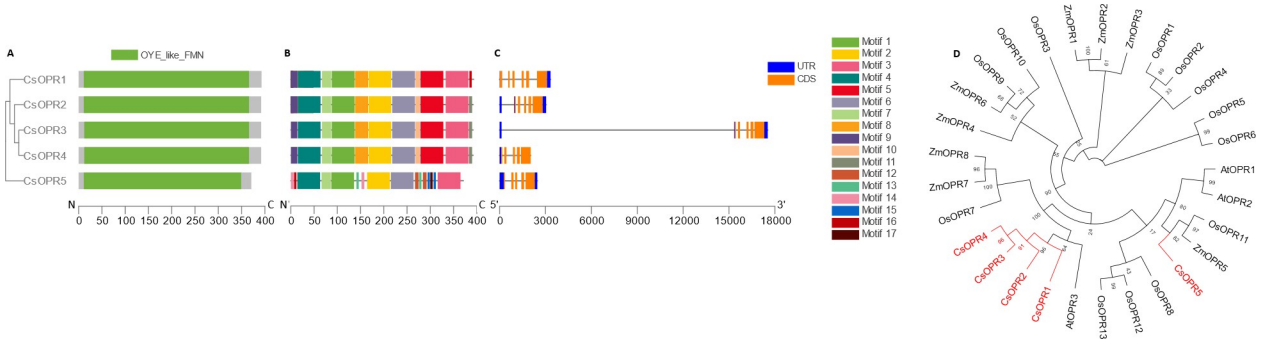

Fig 5. Phylogenetic, genetic, motif, and domain analysis of the CsOPR gene family. (A) Cladogram of peptide sequences and conserved domains. **(B)** Distribution of conserved peptide sequence motifs. Colors are described in legend; x-axis represents length of peptides in amino acids. **(C)** Diagram of genetic structure. Blue bars, orange bars, and gray lines represent untranslated regions, exons, and introns, respectively; x-axis represents length of gene in nucleotides. **(D)** Polar cladogram depicting evolutionary relationship with gene families of selected species. Node labels show confidence values from 1000 bootstrap replications.

https://doi.org/10.1371/journal.pone.0272893.g005

Some LOX, CYP74, and AOC members are syntenic across *Cannabis*, *Arabidopsis*, and tomato

To infer the ancestry of the *C. sativa* oxylipin pathway, a genetic collinearity analysis was performed to compare physical co-localization of oxylipin biosynthetic genes in the genomes of *C. sativa* against two dicot genomes with well characterized oxylipin biosynthetic pathways, *A. thaliana*, and *S. lycopersicum* (tomato) (Fig 6). Remarkably, three LOX genes displayed collinearity across all three species. Of the 9-LOXs, *CsLOX2* was in a syntenic region with *AtLOX1* and *SlLOX5* (also known as TOM*LOXE*). Two 13-LOXs display collinearity, *CsLOX14* with both *AtLOX3* and *AtLOX4* and with *SlLOX4/ LOXD*, while *CsLOX13* was collinear with *AtLOX6* and *SlLOX11*. Two *C. sativa* CYP74 genes were in syntenic regions with tomato genes. *CsAOS2* matched with *SlDES* (also known as *LeDES*) and *CsHPL* matched with both *SlHPL* and *SlAOS3*. Two *CsAOC* genes were collinear with either plant species although with dissimilarities. *CsAOC2* was in a syntenic gene block with *SlAOC* and *CsAOC3* matched with both *AtAOC1* and *AtAOC4*.

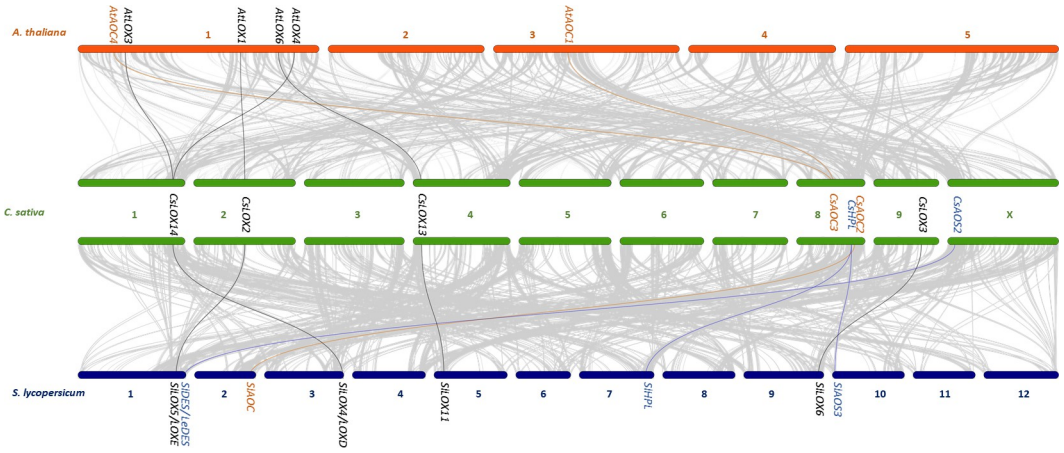

Fig 6. Oxylipin biosynthetic gene collinearity between *A. thaliana*, *C. sativa*, and *S. lycopersicum*. The grey lines represent collinear genetic blocks between the genomes of *A. thaliana* and *C. sativa* and between *C. sativa* and *S. lycospersicum*. Bars represent chromosomes and the black, blue, and orange lines represent the collinear pairs of LOX, CYP74, and AOC gene families, respectively.

https://doi.org/10.1371/journal.pone.0272893.g006

Promoters of *C. sativa* oxylipin biosynthetic genes carry tissue-specific, conditional, and phytohormone-inducible cis-acting regulatory elements (CAREs)

To elucidate the involvement of *Cannabis* oxylipin genes in diverse developmental and stress responses, an *in silico* promoter analysis was conducted to identify cis-regulatory elements involved in plant tissue-specific expression (endosperm, meristem, mesophyll, seed), adaptation to environmental conditions (anaerobic, circadian rhythm, drought, light, and low temperature), and phytohormone signaling, namely, abscisic acid (ABA), gibberellic acid (GA), indole-3-acetic acid (IAA), JA, and salicylic acid (SA).

All promoters varied considerably in the content, arrangement, and position of their CAREs (Fig 7 and S1 Table). Overall, the oxylipin biosynthetic gene promoters possessed CARE motifs with lengths of 8 to 32 nucleotides. For the LOX gene family, the promoter of *CsLOX12* gene was found to contain the most regulatory elements with 32 and followed by *CsLOX16* and *21*, each with 28, while *CsLOX2*, *7*, *11*, and *17* displayed the least, with around 10 each. The *Cannabis*-specific 9-LOX group (CsLOX4-11) displayed the most motifs followed by the amplified GLV-producing 13-LOXs (CsLOX15-21). With the exception of CsLOX5, all contained several regulatory elements involved in conditional responses, though few contained elements involved in tissue expression. CAREs involved in light responses dominated most promoters with all genes having at least three such motifs. Interestingly, CsLOX12 light-responsive motifs constituted over 60% of all its identified motifs. Promoters associated with the presence of phytohormone inducible cis-regulatory elements varies considerably, spanning from 0 to 8 regulatory elements. With the exception of CsLOX2, 4, 7, 8, and 17, all had at least one CARE related to ABA responses. Incidentally, CsLOX2, 4, 7, 8, and 17 were also among

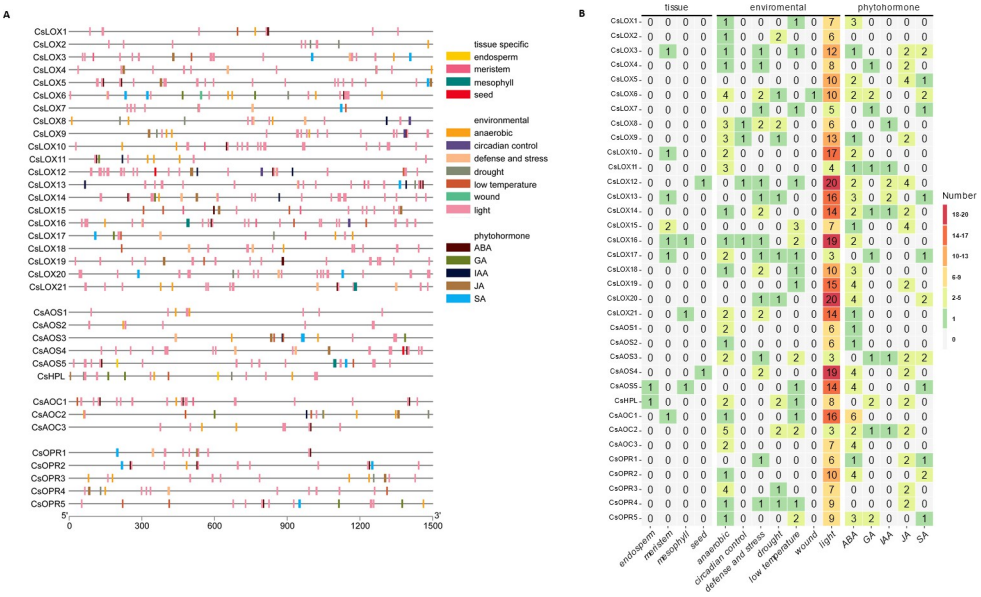

Fig 7. *Cis*-acting regulatory element distribution across *C. sativa* oxylipin biosynthetic gene promoters. (**A**) Physical distribution of motifs throughout a 1.5 kb region upstream of corresponding gene model. Gene symbols are presented on the left with grey line representing promoter regions with motif positions. Legend describes motifs associate with tissue-specific expression, environmental responses, and phytohormone inducibility. (**B**) Summary of *cis*-acting regulatory motif content. Heatmap depicts number of motifs identified in gene promoter region. The y-axis depicts *C. sativa* oxylipin biosynthetic genes and x-axis depicts associated condition for motif. Cell values are number of motifs identified and are colored according to legend.

https://doi.org/10.1371/journal.pone.0272893.g007

the few members that showed motifs involved in GA responses, suggesting a role mediated by ABA-GA antagonism [94]. SA-responsive motifs were limited and predominately associated with the 9-LOXs.

Of the CYP74 gene family, the largest number of CAREs were identified on promoters of CsAOS4 and 5, followed by CsHPL (Fig 7). Relatively few were found on the putative JA-producing CsAOS1, namely those associated with anaerobic conditions, light, and ABA signaling responses. Unlike the pattern observed for LOXs, the disparity between light-related motifs and other CAREs was not as dramatic in the CYP74 family, with the exception of the CsAOS4 and 5 pair. Nearly all CYP74s had ABA-responsive motifs, with the exception of CsAOS3 and CsHPL which were also the only ones to possess GA-related motifs. CsAOS3, 4, and CsHPL each had two JA-related motifs, while CsAOS1 had none; this suggests a limited contribution of positive feedforward control of JA biosynthesis.

Analysis of the AOC gene family found only a single tissue-type related to CAREs across the promoters of all members: CsAOC1 for meristem expression. While non-light conditional-response motifs were the most numerous in CsAOC2 compared to the other two isomers, the opposite was seen for light-responsive motifs, where only three were found in CsAOC2. This was a sharp contrast with CsAOC1, which showed more than twice the number of these CAREs compared to its paralogs (Fig 7). No AOC was found to have SA-related, and only CsAOC2 had JA-related motifs, while all had ABA-related motifs.

Promoters of the OPR gene family contained similar patterns of CAREs compared with the other gene families, albeit with reduced CARE content. No tissue-related CARE was detected for any OPR member. However, all other members possessed motifs for anaerobic responses, with the exception of CsOPR1 (Fig 7). ABA motifs were found in CsOPR1, CsOPR2, and CsOPR5. CsOPR5 was also the only member to show GA motifs, and JA motifs were found in CsOPR1, 3, and 4. The notable difference in CARE patterns found within the JA-producing OPRs (CsOPR1-4), suggests that the 12-OPDA to JA balance is maintained in *Cannabis* via transcriptional control of distinct OPR members responses to the plant's environment and during phytohormone signaling [95].

C. sativa oxylipin biosynthetic genes show tissue-, developmental-, and cultivar-specific expression

Promoter analysis suggested that expression of *C. sativa* oxylipin biosynthetic genes would display distinct patterns. To understand the transcriptional profile of oxylipin biosynthetic genes and to elucidate their role in *Cannabis* development and physiology, the gene expression of 23 tissues from a *C. sativa* transcriptome atlas [72] were examined (S2 Table). Overall, the major contributor associated with levels of expression appeared to be the identity of the specific gene family member, i.e., patterns of expression levels were generally consistent across the tissues examined (Fig 8A). Moreover, several members in all gene families had few if any detected transcripts across all tissues, suggesting a limited role for those isoforms under basal conditions or in the tissues profiled.

Of the 9-LOXs, *CsLOX1*, *2*, *4*, *7* and *8* showed pronounced levels of expression across most tissues. *CsLOX4* is particularly notable as the highest expressed oxylipin biosynthetic gene analyzed, by one order of magnitude, in root and trichome tissues (Fig 8A), highlighting the probable importance of this isoform grouping within the *Cannabis*-specific 9-LOX clade (Fig 2). Curiously, *CsLOX9* and *10* had minimal levels of expression in all but root tissues, where their levels were 20-fold higher compared to other tissues. With respect to the 13-LOXs, with the exception of *CsLOX13* and *18*, all had elevated expression in reproductive-related tissue. However, under these basal conditions, only *CsLOX14* showed modest expression in roots.

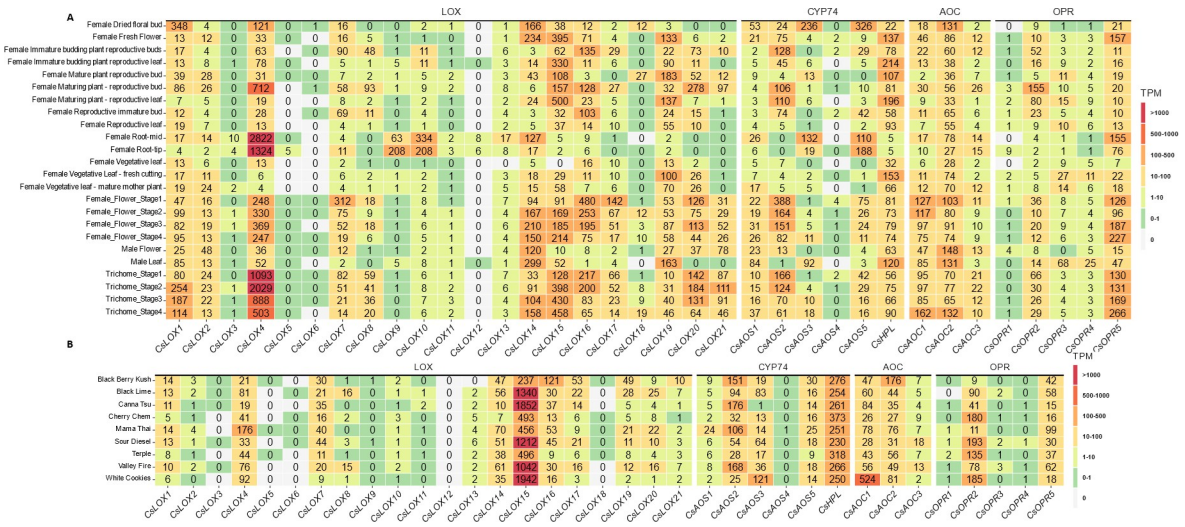

Fig 8. Heatmaps showing expression of oxylipin biosynthetic genes from the *C. sativa* gene expression atlas (A) or female trichomes of diverse marijuana lines (B). Cells values are rounded TPM values and are colored according to the legend.

https://doi.org/10.1371/journal.pone.0272893.g008

Remarkably, despite possessing the greatest number of identified CAREs (Fig 7B), nearly no expression was detected for *CsLOX12* (Fig 8A) which implies a non-basal role for this gene.

In regards to the CYP74-related genes, the likely non-JA producing *CsAOS2* displayed the most abundant expression levels, predominantly in early stages of flower and trichome development (Fig 8A, S3 Fig). The putative JA-producing, *CsAOS1*, also showed its greatest levels of expression in the female flowers, while minimally expressed in other tissues. While *CsAOS5* showed modest levels of expression across tissues, transcripts of its closest paralogue *CsAOS4* were only detected at low levels in few tissues. For the GLV- and cannabinoid-producing *CsHPL*, expression remained consistent across tissues, disregarding low levels in root tissues (Fig 8A). Interestingly, *CsHPL* expression remained relatively consistent across all stages of flower and trichome development (S3 Fig).

In the majority of tissues, *CsAOC2* showed the most uniform levels of expression from this gene family (Fig 8), suggesting this member is the prominent isoform involved in JA biosynthesis under basal conditions. *CsAOC1* and *CsAOC3* showed moderate to modest levels of expression across most tissue types with several exceptions, prompting the idea that these members participate in inducible processes.

Only *CsOPR2 and 5*, displayed mentionable levels of expression. *CsOPR2* transcript levels were an order of magnitude higher than the other Type II paralogs, suggesting this is the major JA-producing isoform under basal conditions (Fig 8). It is also notable that the majority of its expression was in tissues related to flower structures. The sole Type I OPR, *CsOPR5* displayed even greater levels of expression in flower tissues, especially developing trichomes, raising the possibility for the involvement of CsOPR5 in reduction or detoxification of metabolites during trichome development.

To understand the variation in gene expression across *Cannabis* diversity, transcriptomes of trichomes from nine cultivars of mixed ancestry [73] were profiled for their expression of oxylipin biosynthetic genes (S3 Table). With the exception of expression of *CsLOX15*, of which transcript levels showed nearly a bimodal distribution across the cultivar tested, i.e., Black Berry Kush, Cherry Chem, Mamma Thai, and Terple possessed half of the expression compared to the five other lines (Fig 8B). Few differences were observed in the other oxylipin biosynthetic gene expression. In particular, decreased expression was seen in *CsLOX14*, *CsLOX16*,

and CsOPR2 from Cherry Cham, Terple, and Black Berry Kush, respectively, relative to the other *Cannabis* lines. On the other hand, Mama Thai and Black Berry Kush showed elevated levels for transcripts of *CsLOX4* and *CsAOC1*, respectively, and trichomes of White Cookies had increased expression of both *CsAOS3* and *CsAOC1*. Interestingly, in sharp contrast to expression levels seen in the transcriptome atlas, transcripts of *CsLOX15* dominated in the trichomes of these cultivars followed by those of *CsLOX4*. In agreement with the oxylipin-derived hexanoic acid hypothesis [96], the expression of *CsHPL* levels were also two- to 10-fold higher compared to the other CYP74s, likely owed to the selection of these cultivars for high cannabinoid production.

Cannabis oxylipin biosynthetic genes are found in gene networks associated with stress responses, growth, and development

To obtain a more detailed picture of the regulation of the *Cannabis* oxylipin biosynthetic genes, an iterative weighted gene co-expression network analysis was performed, using multi-tissue expression data from the *Cannabis* transcriptome atlas [72]. This analysis revealed that 11 oxylipin biosynthesis genes were found clustering in seven multi-gene modules (Fig 9A), while the rest did not exhibit clustering with other genes, using the data available to us. The four largest modules contained between 1130–1852 genes each, in total containing a regulatory network up to 30% of the *C. sativa* gene models. One of these larger modules contained *CsAOS5*, while the other three modules contained multiple oxylipin biosynthetic genes: *CsLOX3* and *10*, *CsOPR3* and *4*, and *CsLOX5*, *9* and *CsOPR1*. The 15 smallest modules had under 200 genes each and together accounted for only 5% of the *C. sativa* transcriptome.

We also performed functional enrichment analysis of the oxylipin gene-associated co-expression network for Gene Ontology and KEGG identified terms related to molecular functions, biological process, and cellular component orthologs (Fig 9B). Among the top 10 terms

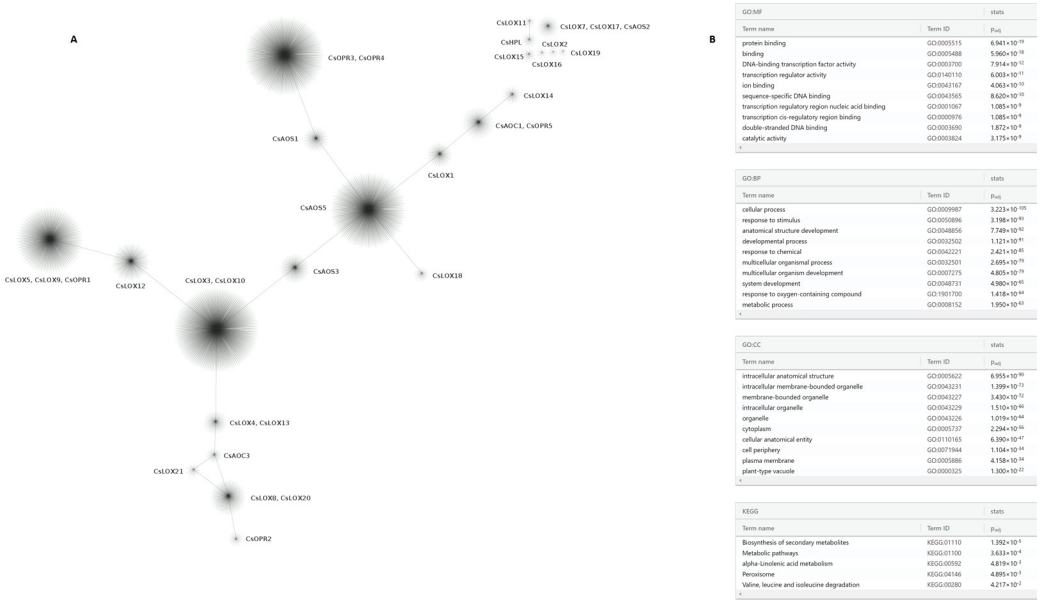

Fig 9. Weighted co-expression genetic network derived from the *C. sativa* transcriptome expression atlas. (A) Clusters represent modules of highly connected genes containing at least one oxylipin biosynthetic gene. **(B)** Functional enrichment analysis of gene modules containing oxylipin biosynthetic genes: Gene Ontologies for Molecular Functions (MF), Biological Processes (BP), and Cellular Components (CC) and KEGG.

https://doi.org/10.1371/journal.pone.0272893.g009

for molecular functions, 60% were related to nucleic acid binding and transcription. Of the biological processes, 80% were related to development or physiological responses. For cellular components, 40% and 30% described organelle- and membrane-related terms, respectively. KEGG terms described secondary metabolism, particularly α-linolenic acid metabolism and branch-chain amino acid degradation. As expected, individual modules were enriched for differential functional terms (S4 Table). Taken together, these results suggest similar members of oxylipin biosynthesis pathways may be regulated in specialized manner, but in general, certain members may be part of transcriptome-wide regulatory networks. Further, focused expression, biochemical, and proteomic experiments will need to be performed to assess the importance of these patterns.

Discussion

Enthusiasm is growing to understand the physiological and ecological functions of plant oxylipins [90]. JA has long served [97] as the model oxylipin, and over the last fifty years, many aspects of its biosynthesis, metabolism, signaling, and activities have started to be defined [98–101]. However, this knowledge has been generated predominantly in the model plant species, *Arabidopsis*, and investigations focusing on oxylipin biology in crop species have been launched only in recent years. Here, we cataloged the major oxylipin biosynthetic genes families of the agro-economically important crop species, *C. sativa*, described their expression patterns, and delineated connections between their putative physiological functions.

LOX gene family

This study adds Cannabaceae to the collection of plant families with described LOX gene families, a group which so far includes Araceae: duckweed [102]; Actinidiaceae: kiwi [103]; Brassicaceae: *Arabidopsis thaliana* [104–106], radish [107], and turnip [108]; Caricaceae: papaya [106]; Cucurbitaceae: cucumber [109, 110], melon [111], and watermelon [112]; Fabaceae: *Medicago truncatula*, peanut [113], and soybean [114]; Malvaceae: cotton [115] Muscaceae: banana [116]; Poaceae: maize [117], rice [105], *Setaria italica* [118], sorghum [119]; Polygonaceae: buckwheat [120]; Rhamnaceae: jujube [121]; Rosaceae: apple [122], peach [123], pear [124]; Salicaceae: poplar [125]; Solanaceae: pepper [126] and tomato [127, 128]; Theaceae: *Camellia sinensis* [129]; and Vitaceae: grape [130].

Of the 21 *C. sativa* LOX isoforms identified (Fig 1), 11 are likely responsible for the production of 9-oxylipins, nine are producers of 13-oxylipins, and one member (CsLOX12) remains to be empirically determined. Of the hallmark 9-LOXs AtLOX1 and AtLOX5, two and one *C. sativa* LOX members grouped with each respectively, while eight formed their own clade. Within 9-LOX phylogenies, monocots typically display their own grouping [102, 116, 118], while the divergence of 9-LOXs in dicots is less common; yet still observed in Cucurbitaceae [111], Salicaceae [125], and Vitaceae [130]. Interestingly, seven members were identified in nearly one large tandem gene array (S1 Fig), which fell within the clade containing both monocot and dicot isoforms required for GLV biosynthesis [45, 131]. Similar substantial gene amplification of this LOX clade has been found to various degrees, in Cucurbitaceae [109–112], Salicaceae [125], and Vitaceae [130]. As *AtLOX2* was not found to be syntenic across the Rosids [106], the gene duplications likely occurred independently in ancestors following the divergence of Rosales, Cucurbitales, Malpighiales, and Vitales.

Proteomic analysis [132] has verified that several lipoxygenases are found with spatial specificity in *Cannabis* flowers and components of their glandular trichomes. Of particular interest was the presence of isoforms from the tandem duplicated 13-LOXs, namely, CsLOX15, 16 and 17 within the trichome head. It is tempting to speculate that these gene duplications may serve

to maintain the pool of hexanoic acid substrate available for cannabinoid biosynthesis. In *Cannabis*, tandem gene arrays have previously been implicated in regulating lipid biosynthesis, particularly the ratios of volatile terpenes that subsequently determines the scent of specific cultivars [133]. This amplification of the 13-LOX paralogues in a tandem gene array may be due to the origin of the representative *C. sativa* genome [57] from CBDRx, a high CBD producing line. The ubiquity of tandem gene arrays among other *Cannabis* species and cultivars remains to be examined, especially in regards to the agronomic characteristics that drive the selection of economically important cultivars. Interestingly, the 9-LOXs, CsLOX4 and 7 were also found within the flower and trichomes where they are likely to contribute to the 9-oxylipin volatiles of *Cannabis* [134].

CYP74 gene family

Despite its importance in oxylipin metabolism, few studies have examined CYP74 gene families from a genome-wide perspective [135–137]. In *C. sativa*, six CYP74 isoforms were identified Specifically CsAOS1 and CsHPL, were distinctly found within the JA- and GLV-producing CYP74 clades, respectively (Fig 3D). Both contained a transient peptide signal sequence predicting localization in plastids (Table 1), although the unique motifs found at their N-terminus suggest an association with different sub-plastid locations. This is similar to tomato where LeAOS was found with the inner chloroplast envelope while LeHPL was targeted to the outer plastid envelope [138]. Four isoforms were found with the CYP74C subfamily, a more irregular group of enzymes with members possessing varying levels of AOS, EAS, and/or HPL activity [139]. It is interesting to note that CsAOS2 was syntenic to the DES of tomato (Fig 6), however, a comprehensive survey and validation of *Cannabis* oxylipins remains to be performed to understand if this species indeed produces divinyl ethers. Ultimately, these isoforms will require biochemical characterization, as even a single amino acid change can result in a new function or protein activity [140, 141]. Four CYP74 peptides (CsAOS1,2,5 and CsHPL) have been detected in association with *Cannabis* flowers, and of these, CsHPL was the only isoform found within trichome heads and stalks [132].

AOC gene family

AOC activity yields the first JA and is the last enzymatic step of JA biosynthesis performed in the chloroplast [101]. Three members of the AOC gene family were identified in *C. sativa*, a number consistent with four of *Arabidopsis* [33], six of soybean [142], and two of maize [26]. Isoforms typically display organ- and tissue-specific expression and function as heterodimers [143]. Only CsAOC2 and CsAOC3 were predicted to localize to plastids (Table 1), supporting the function of these isoforms in JA-biosynthesis. Remarkably, CsAOC3 showed synteny with both *Arabidopsis* (*AtAOC1* and *AtAOC4*) and tomato (*SlAOC*) orthologues. In *Arabidopsis*, heteromers containing AtAOC1 and AtAOC4 display the greatest enzymatic activity [144], suggesting an evolutionary advantage of this conserved genomic region for JA production.

OPR gene family

A larger variability in OPR gene content exists across plant species analyzed so far: three in *Arabidopsis* [38], five in pea [145], five in watermelon [146], eight in maize [147], 10 in cotton [148], 13 in rice [149], and 48 in wheat [150]. This study identified one Type I OPR and four Type II OPRs in the *C. sativa* genome. Both subgroups reduce α, β -unsaturated double bonds and are involved in reactive electrophilic species (RES) detoxification [151, 152]. While Type II OPRs are well-characterized for their peroxisomal role in reducing 12-OPDA to OPC8:0 during JA biosynthesis, Type I OPRs are less understood. They have been shown to reduce 4,

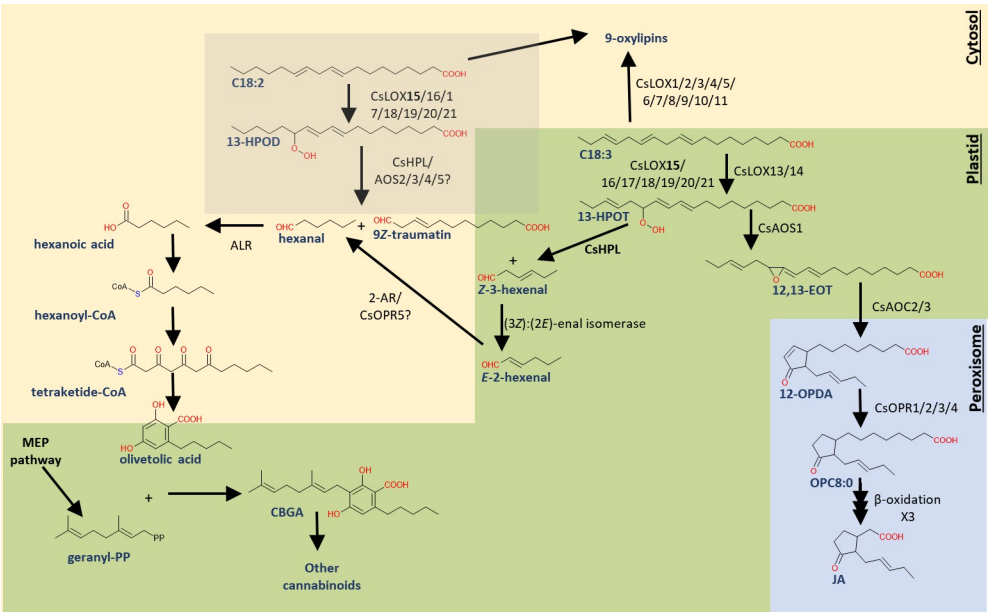

Fig 10. Working model of *C. sativa* oxylipin biosynthetic enzyme isoforms and pathways involved in cannabinoid, GLV, and JA biosynthesis. Abbreviations: [enzymes]: allene oxide cyclase (AOC), allene oxide synthase (AOS), 2-alkynal reductase (2-AR), hydroperoxide lyase (HPL), lipoxygenase (LOX), methylerythritol 4-phosphate pathway (MEP), 12-oxo-phytodienoic reductase (OPR); [metabolites]: (9*Z*, 11*E*, 13*S*, 15*Z*)-12,13-epoxy-9,11,15-octadecatrienoic acid (12,13-EOT), (9*Z*, 11*E*, 13*S*)-13-hydroperoxy-9,11-octadecadienoic acid (13-HPOD), (9*Z*, 11*E*, 13*S*, 15*Z*)-13-hydroperoxy-9,11,15-octadecatrienoic acid (13-HPOT), cannabigerolic acid (CBGA), linoleic acid (C18:2), α-linolenic acid (C18:3), jasmonic acid (JA), 12-oxo-phytodienoic acid (12-OPDA), 3-oxo-2-(2′[*Z*]-pentenyl)-cyclopentane-1-octanoic acid (OPC8:0). The gray box indicates uncertainty in subcellular localization.

https://doi.org/10.1371/journal.pone.0272893.g010

6-trinitrotoluene (TNT) [93] and were recently demonstrated to be involved in producing JA through reduction of an endogenous cyclopentenone JA-analog [42]. Tandem duplication has been implicated as playing a major role in the size of OPR gene families across plant species [153] and interestingly, while all Type II OPRs were found together in a gene cluster, no OPR displayed synteny across the species tested, suggesting OPR gene duplication was a relatively recent event in the *C. sativa* ancestor.

Oxylipins in *Cannabis*

To date, the interaction between the *Cannabis* oxylipin and cannabinoid pathways has largely been overlooked. Several investigations have sought to increase cannabinoid content using JA or methyl-JA treatments on *Cannabis* flowers [154], leaves [155], or cell cultures [156] and have been met with mixed results. Studies that analyze oxylipin levels in *Cannabis* tissues or products have focused on volatiles from above-ground tissues [157], seeds [158], or seed oil [159, 160] as components of their odor profiles. Recently, it was found that sex impacts the distinct oxylipin species that accumulate in the *Cannabis* flower. While male flowers have increased accumulation of the 9-LOX-derived, 9-oxo-octadecadienoic acid, female flowers accumulated higher levels of 12-OPDA [161].

Conclusion

While the LOX pathway is the hypothetical origin of the hexanoic acid moiety used for cannabinoid biosynthesis [12, 19, 24, 25, 96], the precise mechanisms for its production are largely unknown. Here, we provide a comprehensive description of the *C. sativa* LOX pathway,

including the major oxylipin biosynthetic gene families, to establish a working model (Fig 10) for further investigations.

Within this context, it will become important to understand the co-localization of the substrates with their corresponding enzymes. LOX activity depends on a 1,4-dipentadiene structure found in either C18:2 or C18:3 [27], both of which, in tomato, account for the most abundant fatty acids in its trichomes [162]. However, while HPL-cleavage of 13-hydroperoxydienoic acid would generate a statured C_6-aldehyde, the GLV-producing 13-LOXs and HPL are likely localized to the C18:3-rich chloroplasts [163, 164]. Additionally, the GLV-producing AtLOX2 oxygenates C18:3 more efficiently than C18:2 [104], which together may explain why unsaturated GLVs prevail as the major C_6 volatile in plants [165].

Enzymatic production of hexanoic acid from the C18:3 HPL-product, *Z*-3-hexenal is unexplored, but would reasonably require distinct enzymatic reactions. Chemical or enzymatic isomerization by (3Z):(2E)-enal isomerase would generate (2*E*)-hexenal [46, 55] which could be reduced to hexanal by 2-alkenal reductase [166] or by OPR [167]. The conversation of the fatty aldehyde to fatty acid likely requires an aldehyde dehydrogenase [168], the product of which would be readily diffused across cell membranes [169]. In an alternative scenario, 13-LOX may oxygenate C18:2 directly, however this would presumably require the cytosolic localization of both 13-LOX and HPL. A 13-LOX isoform in melon was shown to have preference for C18:2 and localized to non-chloroplast organelles [170]. This strategy would take advantage of the relatively high C18:2 content in the inflorescences of some *Cannabis* cultivars [171].

Understanding and applying knowledge of the *Cannabis* oxylipin biosynthetic pathway is expected to provide novel environmentally friendly approaches towards improving the crop and its desirable consumer traits. Similar technologies in maize and soybeans in development aim at increasing disease resistance [172], drought tolerance [173], and seed flavor [174]. Exploiting the diversity in *Cannabis* cultivars via oxylipin biosynthetic gene expression and variability in the predominant oxylipin biosynthetic pathway branch across cultivars and species (e.g., *C. sativa* vs *C. indica*) should also provide opportunities for manipulating cannabinoid content and other traits through marker-assisted selection or identification of superior alleles.

Supporting information

S1 Fig. Regions of duplicated LOX genes on *C. sativa* Chromosomes 2 and 9.
(TIF)

S2 Fig. Regions of duplicated *OPR*, *AOS*, and *AOC* genes on *C. sativa* Chromosomes 1, 8, and X.
(TIF)

S3 Fig. Expression of oxylipin biosynthetic genes across four developmental stages in *C. sativa* flowers and trichomes.
(TIF)

S1 Table. Promoter analysis.
(XLSX)

S2 Table. Transcriptome atlas RNAseqs.
(XLSX)

S3 Table. Trichome RNAseq.
(XLSX)

S4 Table. Gene network analysis.
(XLSX)

Acknowledgments

Thank you to Dr. Michael Kolomiets for helpful discussions and Dr. Michael Osier for the use of computational resources.

Author Contributions

Conceptualization: Eli J. Borrego.

Data curation: Eli J. Borrego.

Formal analysis: Eli J. Borrego, James Taylor, Elida M. Espinoza.

Funding acquisition: Eli J. Borrego.

Investigation: Eli J. Borrego, Mariah Robertson.

Methodology: Eli J. Borrego.

Project administration: Eli J. Borrego.

Resources: Eli J. Borrego.

Software: Eli J. Borrego.

Supervision: Eli J. Borrego.

Validation: Eli J. Borrego.

Visualization: Eli J. Borrego, James Taylor.

Writing – original draft: Eli J. Borrego.

Writing – review & editing: Eli J. Borrego, Zachary Schultzhaus, Elida M. Espinoza.

References

1. Bonini SA, Premoli M, Tambaro S, Kumar A, Maccarinelli G, Memo M, et al. Cannabis sativa: A comprehensive ethnopharmacological review of a medicinal plant with a long history. J Ethnopharmacol. 2018; 227:300–15. https://doi.org/10.1016/j.jep.2018.09.004 PMID: 30205181
2. Kovalchuk I, Pellino M, Rigault P, van Velzen R, Ebersbach J, Ashnest JR, et al. The Genomics of Cannabis and Its Close Relatives. Annu Rev Plant Biol. 2020; 71:713–39. https://doi.org/10.1146/annurev-arplant-081519-040203 PMID: 32155342
3. de la Fuente A, Zamberlan F, Ferrán AS, Carrillo F, Tagliazucchi E, Pallavicini C. Relationship among subjective responses, flavor, and chemical composition across more than 800 commercial cannabis varieties. Journal of cannabis research. 2020; 2(1):1–18. https://doi.org/10.1186/s42238-020-00028-y PMID: 33526118
4. Torkamaneh D, Jones AMP. Cannabis, the multibillion dollar plant that no genebank wanted. Genome. 2021; 99(999):1–5. https://doi.org/10.1139/gen-2021-0016 PMID: 34242522
5. Rehman M, Fahad S, Du G, Cheng X, Yang Y, Tang K, et al. Evaluation of hemp (Cannabis sativa L.) as an industrial crop: a review. Environ Sci Pollut Res Int. 2021; 28(38):52832–43. https://doi.org/10.1007/s11356-021-16264-5 PMID: 34476693
6. Callaway JC. Hempseed as a nutritional resource: An overview. Euphytica. 2004; 140(1–2):65–72.
7. Duque Schumacher AG, Pequito S, Pazour J. Industrial hemp fiber: A sustainable and economical alternative to cotton. Journal of Cleaner Production. 2020; 268:122180.
8. Finnan J, Styles D. Hemp: A more sustainable annual energy crop for climate and energy policy. Energy Policy. 2013; 58:152–62.

9. Citti C, Braghiroli D, Vandelli MA, Cannazza G. Pharmaceutical and biomedical analysis of cannabinoids: A critical review. J Pharm Biomed Anal. 2018; 147:565–79. https://doi.org/10.1016/j.jpba.2017.06.003 PMID: 28641906
10. Keul A, Eisenhauer B. Making the high country: cannabis tourism in Colorado USA. Annals of Leisure Research. 2018; 22(2):140–60.
11. Peng H, Shahidi F. Cannabis and Cannabis Edibles: A Review. J Agric Food Chem. 2021; 69 (6):1751–74. https://doi.org/10.1021/acs.jafc.0c07472 PMID: 33555188
12. Gulck T, Moller BL. Phytocannabinoids: Origins and Biosynthesis. Trends Plant Sci. 2020; 25 (10):985–1004. https://doi.org/10.1016/j.tplants.2020.05.005 PMID: 32646718
13. Lange BM, Zager JJ. Comprehensive inventory of cannabinoids in Cannabis sativa L.: Can we connect genotype and chemotype? Phytochemistry Reviews. 2021:1–41.
14. Flores-Sanchez IJ, Verpoorte R. Secondary metabolism in cannabis. Phytochemistry reviews. 2008; 7 (3):615–39.
15. Iseger TA, Bossong MG. A systematic review of the antipsychotic properties of cannabidiol in humans. Schizophr Res. 2015; 162(1–3):153–61. https://doi.org/10.1016/j.schres.2015.01.033 PMID: 25667194
16. Mechoulam R, Parker LA. The endocannabinoid system and the brain. Annu Rev Psychol. 2013; 64:21–47. https://doi.org/10.1146/annurev-psych-113011-143739 PMID: 22804774
17. Toth JA, Stack GM, Cala AR, Carlson CH, Wilk RL, Crawford JL, et al. Development and validation of genetic markers for sex and cannabinoid chemotype in Cannabis sativa L. Global Change Biology Bioenergy. 2020; 12(3):213–22.
18. Johnson MS, Wallace JG. Genomic and Chemical Diversity of Commercially Available High-CBD Industrial Hemp Accessions. Front Genet. 2021; 12(1160):682475. https://doi.org/10.3389/fgene.2021.682475 PMID: 34306025
19. Blatt-Janmaat K, Qu Y. The Biochemistry of Phytocannabinoids and Metabolic Engineering of Their Production in Heterologous Systems. Int J Mol Sci. 2021; 22(5):2454. https://doi.org/10.3390/ijms22052454 PMID: 33671077
20. Luo X, Reiter MA, d'Espaux L, Wong J, Denby CM, Lechner A, et al. Complete biosynthesis of cannabinoids and their unnatural analogues in yeast. Nature. 2019; 567(7746):123–6. https://doi.org/10.1038/s41586-019-0978-9 PMID: 30814733
21. Tahir MN, Shahbazi F, Rondeau-Gagne S, Trant JF. The biosynthesis of the cannabinoids. J Cannabis Res. 2021; 3(1):7. https://doi.org/10.1186/s42238-021-00062-4 PMID: 33722296
22. Hanus LO, Meyer SM, Munoz E, Taglialatela-Scafati O, Appendino G. Phytocannabinoids: a unified critical inventory. Nat Prod Rep. 2016; 33(12):1357–92. https://doi.org/10.1039/c6np00074f PMID: 27722705
23. Tan Z, Clomburg JM, Gonzalez R. Synthetic Pathway for the Production of Olivetolic Acid in Escherichia coli. ACS Synth Biol. 2018; 7(8):1886–96. https://doi.org/10.1021/acssynbio.8b00075 PMID: 29976061
24. Livingston SJ, Quilichini TD, Booth JK, Wong DCJ, Rensing KH, Laflamme-Yonkman J, et al. Cannabis glandular trichomes alter morphology and metabolite content during flower maturation. Plant J. 2020; 101(1):37–56. https://doi.org/10.1111/tpj.14516 PMID: 31469934
25. Stout JM, Boubakir Z, Ambrose SJ, Purves RW, Page JE. The hexanoyl-CoA precursor for cannabinoid biosynthesis is formed by an acyl-activating enzyme in Cannabis sativa trichomes. The Plant Journal. 2012; 71(3):353–65. https://doi.org/10.1111/j.1365-313X.2012.04949.x PMID: 22353623
26. Borrego EJ, Kolomiets MV. Synthesis and Functions of Jasmonates in Maize. Plants (Basel). 2016; 5 (4):41. https://doi.org/10.3390/plants5040041 PMID: 27916835
27. Feussner I, Wasternack C. The lipoxygenase pathway. Annu Rev Plant Biol. 2002; 53(1):275–97. https://doi.org/10.1146/annurev.arplant.53.100301.135248 PMID: 12221977
28. Yan Y, Christensen S, Isakeit T, Engelberth J, Meeley R, Hayward A, et al. Disruption of OPR7 and OPR8 reveals the versatile functions of jasmonic acid in maize development and defense. Plant Cell. 2012; 24(4):1420–36. https://doi.org/10.1105/tpc.111.094151 PMID: 22523204
29. Yan Y, Borrego E, Kolomiets MV. Jasmonate biosynthesis, perception and function in plant development and stress responses. Lipid metabolism InTech. 2013:393–442.
30. Wasternack C. Jasmonates: an update on biosynthesis, signal transduction and action in plant stress response, growth and development. Ann Bot. 2007; 100(4):681–97. https://doi.org/10.1093/aob/mcm079 PMID: 17513307
31. Laudert D, Pfannschmidt U, Lottspeich F, Hollander-Czytko H, Weiler EW. Cloning, molecular and functional characterization of Arabidopsis thaliana allene oxide synthase (CYP 74), the first enzyme of

the octadecanoid pathway to jasmonates. Plant Mol Biol. 1996; 31(2):323–35. https://doi.org/10.1007/BF00021793 PMID: 8756596

32. Park JH, Halitschke R, Kim HB, Baldwin IT, Feldmann KA, Feyereisen R. A knock-out mutation in allene oxide synthase results in male sterility and defective wound signal transduction in Arabidopsis due to a block in jasmonic acid biosynthesis. The Plant Journal. 2002; 31(1):1–12. https://doi.org/10.1046/j.1365-313x.2002.01328.x PMID: 12100478

33. Stenzel I, Hause B, Miersch O, Kurz T, Maucher H, Weichert H, et al. Jasmonate biosynthesis and the allene oxide cyclase family of Arabidopsis thaliana. Plant Mol Biol. 2003; 51(6):895–911. https://doi.org/10.1023/a:1023049319723 PMID: 12777050

34. Pollmann S, Springer A, Rustgi S, von Wettstein D, Kang C, Reinbothe C, et al. Substrate channeling in oxylipin biosynthesis through a protein complex in the plastid envelope of Arabidopsis thaliana. J Exp Bot. 2019; 70(5):1483–95. https://doi.org/10.1093/jxb/erz015 PMID: 30690555

35. Park SW, Li W, Viehhauser A, He B, Kim S, Nilsson AK, et al. Cyclophilin 20–3 relays a 12-oxo-phytodienoic acid signal during stress responsive regulation of cellular redox homeostasis. Proc Natl Acad Sci U S A. 2013; 110(23):9559–64. https://doi.org/10.1073/pnas.1218872110 PMID: 23671085

36. Stintzi A, Weber H, Reymond P, Browse J, Farmer EE. Plant defense in the absence of jasmonic acid: the role of cyclopentenones. Proc Natl Acad Sci U S A. 2001; 98(22):12837–42. https://doi.org/10.1073/pnas.211311098 PMID: 11592974

37. Wang KD, Borrego EJ, Kenerley CM, Kolomiets MV. Oxylipins Other Than Jasmonic Acid Are Xylem-Resident Signals Regulating Systemic Resistance Induced by Trichoderma virens in Maize. Plant Cell. 2020; 32(1):166–85. https://doi.org/10.1105/tpc.19.00487 PMID: 31690653

38. Mussig C, Biesgen C, Lisso J, Uwer U, Weiler EW, Altmann T. A novel stress-inducible 12-oxophytodienoate reductase from Arabidopsis thaliana provides a potential link between Brassinosteroid-action and Jasmonic-acid synthesis. Journal of Plant Physiology. 2000; 157(2):143–52.

39. Stintzi A, Browse J. The Arabidopsis male-sterile mutant, opr3, lacks the 12-oxophytodienoic acid reductase required for jasmonate synthesis. Proc Natl Acad Sci U S A. 2000; 97(19):10625–30. https://doi.org/10.1073/pnas.190264497 PMID: 10973494

40. Vick BA, Zimmerman DC. Biosynthesis of jasmonic Acid by several plant species. Plant Physiol. 1984; 75(2):458–61. https://doi.org/10.1104/pp.75.2.458 PMID: 16663643

41. Wasternack C, Hause B. A Bypass in Jasmonate Biosynthesis—the OPR3-independent Formation. Trends Plant Sci. 2018; 23(4):276–9. https://doi.org/10.1016/j.tplants.2018.02.011 PMID: 29530379

42. Chini A, Monte I, Zamarreno AM, Hamberg M, Lassueur S, Reymond P, et al. An OPR3-independent pathway uses 4,5-didehydrojasmonate for jasmonate synthesis. Nat Chem Biol. 2018; 14(2):171–8. https://doi.org/10.1038/nchembio.2540 PMID: 29291349

43. Weber H, Vick BA, Farmer EE. Dinor-oxo-phytodienoic acid: a new hexadecanoid signal in the jasmonate family. Proc Natl Acad Sci U S A. 1997; 94(19):10473–8. https://doi.org/10.1073/pnas.94.19.10473 PMID: 9294235

44. Fonseca S, Chini A, Hamberg M, Adie B, Porzel A, Kramell R, et al. (+)-7-iso-Jasmonoyl-L-isoleucine is the endogenous bioactive jasmonate. Nature chemical biology. 2009; 5(5):344–50. https://doi.org/10.1038/nchembio.161 PMID: 19349968

45. Christensen SA, Nemchenko A, Borrego E, Murray I, Sobhy IS, Bosak L, et al. The maize lipoxygenase, Zm LOX 10, mediates green leaf volatile, jasmonate and herbivore-induced plant volatile production for defense against insect attack. The Plant Journal. 2013; 74(1):59–73. https://doi.org/10.1111/tpj.12101 PMID: 23279660

46. Ameye M, Allmann S, Verwaeren J, Smagghe G, Haesaert G, Schuurink RC, et al. Green leaf volatile production by plants: a meta-analysis. New Phytol. 2018; 220(3):666–83. https://doi.org/10.1111/nph.14671 PMID: 28665020

47. Sugimoto K, Iijima Y, Takabayashi J, Matsui K. Processing of Airborne Green Leaf Volatiles for Their Glycosylation in the Exposed Plants. Front Plant Sci. 2021; 12(2514):721572. https://doi.org/10.3389/fpls.2021.721572 PMID: 34868107

48. Bate NJ, Sivasankar S, Moxon C, Riley JM, Thompson JE, Rothstein SJ. Molecular characterization of an Arabidopsis gene encoding hydroperoxide lyase, a cytochrome P-450 that is wound inducible. Plant Physiol. 1998; 117(4):1393–400. https://doi.org/10.1104/pp.117.4.1393 PMID: 9701595

49. Matsui K, Wilkinson J, Hiatt B, Knauf V, Kajiwara T. Molecular cloning and expression of Arabidopsis fatty acid hydroperoxide lyase. Plant Cell Physiol. 1999; 40(5):477–81. https://doi.org/10.1093/oxfordjournals.pcp.a029567 PMID: 10427771

50. Duan H, Huang MY, Palacio K, Schuler MA. Variations in CYP74B2 (hydroperoxide lyase) gene expression differentially affect hexenal signaling in the Columbia and Landsberg erecta ecotypes of

Arabidopsis. Plant Physiol. 2005; 139(3):1529–44. https://doi.org/10.1104/pp.105.067249 PMID: 16258015

51. Kallenbach M, Gilardoni PA, Allmann S, Baldwin IT, Bonaventure G. C12 derivatives of the hydroperoxide lyase pathway are produced by product recycling through lipoxygenase-2 in Nicotiana attenuata leaves. New Phytologist. 2011; 191(4):1054–68. https://doi.org/10.1111/j.1469-8137.2011.03767.x PMID: 21615741

52. Nakashima A, von Reuss SH, Tasaka H, Nomura M, Mochizuki S, Iijima Y, et al. Traumatin- and dinortraumatin-containing galactolipids in Arabidopsis: their formation in tissue-disrupted leaves as counterparts of green leaf volatiles. J Biol Chem. 2013; 288(36):26078–88. https://doi.org/10.1074/jbc.M113.487959 PMID: 23888054

53. Tanaka T, Ikeda A, Shiojiri K, Ozawa R, Shiki K, Nagai-Kunihiro N, et al. Identification of a Hexenal Reductase That Modulates the Composition of Green Leaf Volatiles. Plant Physiol. 2018; 178(2):552–64. https://doi.org/10.1104/pp.18.00632 PMID: 30126866

54. D'Auria JC, Pichersky E, Schaub A, Hansel A, Gershenzon J. Characterization of a BAHD acyltransferase responsible for producing the green leaf volatile (Z)-3-hexen-1-yl acetate in Arabidopsis thaliana. Plant J. 2007; 49(2):194–207. https://doi.org/10.1111/j.1365-313X.2006.02946.x PMID: 17163881

55. Kunishima M, Yamauchi Y, Mizutani M, Kuse M, Takikawa H, Sugimoto Y. Identification of (Z)-3:(E)-2-Hexenal Isomerases Essential to the Production of the Leaf Aldehyde in Plants. J Biol Chem. 2016; 291(27):14023–33. https://doi.org/10.1074/jbc.M116.726687 PMID: 27129773

56. Spyropoulou EA, Dekker HL, Steemers L, van Maarseveen JH, de Koster CG, Haring MA, et al. Identification and Characterization of (3Z):(2E)-Hexenal Isomerases from Cucumber. Front Plant Sci. 2017; 8:1342. https://doi.org/10.3389/fpls.2017.01342 PMID: 28824678

57. Grassa CJ, Weiblen GD, Wenger JP, Dabney C, Poplawski SG, Timothy Motley S, et al. A new Cannabis genome assembly associates elevated cannabidiol (CBD) with hemp introgressed into marijuana. New Phytol. 2021; 230(4):1665–79. https://doi.org/10.1111/nph.17243 PMID: 33521943

58. Rangwala SH, Kuznetsov A, Ananiev V, Asztalos A, Borodin E, Evgeniev V, et al. Accessing NCBI data using the NCBI Sequence Viewer and Genome Data Viewer (GDV). Genome Res. 2021; 31(1):159–69. https://doi.org/10.1101/gr.266932.120 PMID: 33239395

59. Lu S, Wang J, Chitsaz F, Derbyshire MK, Geer RC, Gonzales NR, et al. CDD/SPARCLE: the conserved domain database in 2020. Nucleic Acids Res. 2020; 48(D1):D265–D8. https://doi.org/10.1093/nar/gkz991 PMID: 31777944

60. Marchler-Bauer A, Lu S, Anderson JB, Chitsaz F, Derbyshire MK, DeWeese-Scott C, et al. CDD: a Conserved Domain Database for the functional annotation of proteins. Nucleic Acids Res. 2011; 39(Database issue):D225–9. https://doi.org/10.1093/nar/gkq1189 PMID: 21109532

61. Bailey TL, Elkan C. Fitting a mixture model by expectation maximization to discover motifs in bipolymers. 1994.

62. Bailey TL, Johnson J, Grant CE, Noble WS. The MEME Suite. Nucleic Acids Res. 2015; 43(W1):W39–49. https://doi.org/10.1093/nar/gkv416 PMID: 25953851

63. Almagro Armenteros JJ, Sønderby CK, Sønderby SK, Nielsen H, Winther O. DeepLoc: prediction of protein subcellular localization using deep learning. Bioinformatics. 2017; 33(21):3387–95. https://doi.org/10.1093/bioinformatics/btx431 PMID: 29036616

64. Sperschneider J, Catanzariti AM, DeBoer K, Petre B, Gardiner DM, Singh KB, et al. LOCALIZER: subcellular localization prediction of both plant and effector proteins in the plant cell. Sci Rep. 2017; 7(1):44598. https://doi.org/10.1038/srep44598 PMID: 28300209

65. Sahu SS, Loaiza CD, Kaundal R. Plant-mSubP: a computational framework for the prediction of single-and multi-target protein subcellular localization using integrated machine-learning approaches. AoB Plants. 2020; 12(3):plz068. https://doi.org/10.1093/aobpla/plz068 PMID: 32528639

66. Almagro Armenteros JJ, Salvatore M, Emanuelsson O, Winther O, von Heijne G, Elofsson A, et al. Detecting sequence signals in targeting peptides using deep learning. Life Sci Alliance. 2019; 2(5). https://doi.org/10.26508/lsa.201900429 PMID: 31570514

67. Katoh K, Rozewicki J, Yamada KD. MAFFT online service: multiple sequence alignment, interactive sequence choice and visualization. Brief Bioinform. 2019; 20(4):1160–6. https://doi.org/10.1093/bib/bbx108 PMID: 28968734

68. Kuraku S, Zmasek CM, Nishimura O, Katoh K. aLeaves facilitates on-demand exploration of metazoan gene family trees on MAFFT sequence alignment server with enhanced interactivity. Nucleic Acids Res. 2013; 41(Web Server issue):W22–8. https://doi.org/10.1093/nar/gkt389 PMID: 23677614

69. Chen C, Chen H, Zhang Y, Thomas HR, Frank MH, He Y, et al. TBtools: An Integrative Toolkit Developed for Interactive Analyses of Big Biological Data. Mol Plant. 2020; 13(8):1194–202. https://doi.org/10.1016/j.molp.2020.06.009 PMID: 32585190

70. Lescot M, Dehais P, Thijs G, Marchal K, Moreau Y, Van de Peer Y, et al. PlantCARE, a database of plant cis-acting regulatory elements and a portal to tools for in silico analysis of promoter sequences. Nucleic Acids Res. 2002; 30(1):325–7. https://doi.org/10.1093/nar/30.1.325 PMID: 11752327

71. Wang Y, Tang H, Debarry JD, Tan X, Li J, Wang X, et al. MCScanX: a toolkit for detection and evolutionary analysis of gene synteny and collinearity. Nucleic Acids Res. 2012; 40(7):e49. https://doi.org/10.1093/nar/gkr1293 PMID: 22217600

72. Braich S, Baillie RC, Jewell LS, Spangenberg GC, Cogan NOI. Generation of a Comprehensive Transcriptome Atlas and Transcriptome Dynamics in Medicinal Cannabis. Sci Rep. 2019; 9(1):16583. https://doi.org/10.1038/s41598-019-53023-6 PMID: 31719627

73. Zager JJ, Lange I, Srividya N, Smith A, Lange BM. Gene Networks Underlying Cannabinoid and Terpenoid Accumulation in Cannabis. Plant Physiol. 2019; 180(4):1877–97. https://doi.org/10.1104/pp.18.01506 PMID: 31138625

74. Chen S, Zhou Y, Chen Y, Gu J. fastp: an ultra-fast all-in-one FASTQ preprocessor. Bioinformatics. 2018; 34(17):i884–i90. https://doi.org/10.1093/bioinformatics/bty560 PMID: 30423086

75. Patro R, Duggal G, Love MI, Irizarry RA, Kingsford C. Salmon provides fast and bias-aware quantification of transcript expression. Nat Methods. 2017; 14(4):417–9. https://doi.org/10.1038/nmeth.4197 PMID: 28263959

76. Langfelder P, Horvath S. WGCNA: an R package for weighted correlation network analysis. BMC Bioinformatics. 2008; 9(1):559.

77. Greenfest-Allen E, Cartailler J-P, Magnuson MA, Stoeckert CJ. iterativeWGCNA: iterative refinement to improve module detection from WGCNA co-expression networks. bioRxiv. 2017:234062.

78. Shannon P, Markiel A, Ozier O, Baliga NS, Wang JT, Ramage D, et al. Cytoscape: a software environment for integrated models of biomolecular interaction networks. Genome Res. 2003; 13(11):2498–504. https://doi.org/10.1101/gr.1239303 PMID: 14597658

79. Raudvere U, Kolberg L, Kuzmin I, Arak T, Adler P, Peterson H, et al. g:Profiler: a web server for functional enrichment analysis and conversions of gene lists (2019 update). Nucleic Acids Res. 2019; 47(W1):W191–W8. https://doi.org/10.1093/nar/gkz369 PMID: 31066453

80. Van Bel M, Silvestri F, Weitz EM, Kreft L, Botzki A, Coppens F, et al. PLAZA 5.0: extending the scope and power of comparative and functional genomics in plants. Nucleic Acids Res. 2022; 50(D1):D1468–D74. https://doi.org/10.1093/nar/gkab1024 PMID: 34747486

81. Kanehisa M. Toward understanding the origin and evolution of cellular organisms. Protein Sci. 2019; 28(11):1947–51. https://doi.org/10.1002/pro.3715 PMID: 31441146

82. Kanehisa M, Furumichi M, Sato Y, Ishiguro-Watanabe M, Tanabe M. KEGG: integrating viruses and cellular organisms. Nucleic Acids Res. 2021; 49(D1):D545–D51. https://doi.org/10.1093/nar/gkaa970 PMID: 33125081

83. Kanehisa M, Goto S. KEGG: kyoto encyclopedia of genes and genomes. Nucleic Acids Res. 2000; 28(1):27–30. https://doi.org/10.1093/nar/28.1.27 PMID: 10592173

84. Ashburner M, Ball CA, Blake JA, Botstein D, Butler H, Cherry JM, et al. Gene ontology: tool for the unification of biology. The Gene Ontology Consortium. Nat Genet. 2000; 25(1):25–9. https://doi.org/10.1038/75556 PMID: 10802651

85. Gene Ontology C. The Gene Ontology resource: enriching a GOld mine. Nucleic Acids Res. 2021; 49(D1):D325–D34. https://doi.org/10.1093/nar/gkaa1113 PMID: 33290552

86. Majorek KA, Dunin-Horkawicz S, Steczkiewicz K, Muszewska A, Nowotny M, Ginalski K, et al. The RNase H-like superfamily: new members, comparative structural analysis and evolutionary classification. Nucleic Acids Res. 2014; 42(7):4160–79. https://doi.org/10.1093/nar/gkt1414 PMID: 24464998

87. Xiong Y, Eickbush TH. Origin and evolution of retroelements based upon their reverse transcriptase sequences. EMBO J. 1990; 9(10):3353–62. https://doi.org/10.1002/j.1460-2075.1990.tb07536.x PMID: 1698615

88. Farmaki T, Sanmartin M, Jimenez P, Paneque M, Sanz C, Vancanneyt G, et al. Differential distribution of the lipoxygenase pathway enzymes within potato chloroplasts. J Exp Bot. 2007; 58(3):555–68. https://doi.org/10.1093/jxb/erl230 PMID: 17210991

89. Mikulska-Ruminska K, Shrivastava I, Krieger J, Zhang S, Li H, Bayir H, et al. Characterization of Differential Dynamics, Specificity, and Allostery of Lipoxygenase Family Members. J Chem Inf Model. 2019; 59(5):2496–508. https://doi.org/10.1021/acs.jcim.9b00006 PMID: 30762363

90. Wasternack C, Feussner I. The Oxylipin Pathways: Biochemistry and Function. Annu Rev Plant Biol. 2018; 69:363–86.

91. Toporkova YY, Smirnova EO, Iljina TM, Mukhtarova LS, Gorina SS, Grechkin AN. The CYP74B and CYP74D divinyl ether synthases possess a side hydroperoxide lyase and epoxyalcohol synthase activities that are enhanced by the site-directed mutagenesis. Phytochemistry. 2020; 179:112512. https://doi.org/10.1016/j.phytochem.2020.112512 PMID: 32927248

92. Li JW, Guang YL, Yang YX, Zhou Y. Identification and Expression Analysis of Two allene oxide cyclase (AOC) Genes in Watermelon. Agriculture-Basel. 2019; 9(10):225.

93. Beynon ER, Symons ZC, Jackson RG, Lorenz A, Rylott EL, Bruce NC. The role of oxophytodienoate reductases in the detoxification of the explosive 2,4,6-trinitrotoluene by Arabidopsis. Plant Physiol. 2009; 151(1):253–61. https://doi.org/10.1104/pp.109.141598 PMID: 19605548

94. Liu X, Hou X. Antagonistic Regulation of ABA and GA in Metabolism and Signaling Pathways. Front Plant Sci. 2018; 9:251. https://doi.org/10.3389/fpls.2018.00251 PMID: 29535756

95. Park S, Liu W. 12-oxo-phytodienoic acid: a fuse and/or switch of plant growth and defense responses? Frontiers in Plant Science. 2021:1687. https://doi.org/10.3389/fpls.2021.724079 PMID: 34490022

96. van Bakel H, Stout JM, Cote AG, Tallon CM, Sharpe AG, Hughes TR, et al. The draft genome and transcriptome of Cannabis sativa. Genome Biol. 2011; 12(10):R102. https://doi.org/10.1186/gb-2011-12-10-r102 PMID: 22014239

97. Aldridge DC, Galt S, Giles D, Turner WB. Metabolites of Lasiodiplodia theobromae. Journal of the Chemical Society C: Organic. 1971(9):1623-&.

98. Huang H, Liu B, Liu L, Song S. Jasmonate action in plant growth and development. J Exp Bot. 2017; 68(6):1349–59. https://doi.org/10.1093/jxb/erw495 PMID: 28158849

99. Howe GA, Major IT, Koo AJ. Modularity in Jasmonate Signaling for Multistress Resilience. Annu Rev Plant Biol. 2018; 69:387–415. https://doi.org/10.1146/annurev-arplant-042817-040047 PMID: 29539269

100. Heitz T, Smirnova E, Marquis V, Poirier L. Metabolic Control within the Jasmonate Biochemical Pathway. Plant Cell Physiol. 2019; 60(12):2621–8. https://doi.org/10.1093/pcp/pcz172 PMID: 31504918

101. Wasternack C, Hause B. Jasmonates: biosynthesis, perception, signal transduction and action in plant stress response, growth and development. An update to the 2007 review in Annals of Botany. Ann Bot. 2013; 111(6):1021–58. https://doi.org/10.1093/aob/mct067 PMID: 23558912

102. Upadhyay RK, Edelman M, Mattoo AK. Identification, Phylogeny, and Comparative Expression of the Lipoxygenase Gene Family of the Aquatic Duckweed, Spirodela polyrhiza, during Growth and in Response to Methyl Jasmonate and Salt. Int J Mol Sci. 2020; 21(24):9527. https://doi.org/10.3390/ijms21249527 PMID: 33333747

103. Zhang B, Chen K, Bowen J, Allan A, Espley R, Karunairetnam S, et al. Differential expression within the LOX gene family in ripening kiwifruit. J Exp Bot. 2006; 57(14):3825–36. https://doi.org/10.1093/jxb/erl151 PMID: 17032731

104. Bannenberg G, Martinez M, Hamberg M, Castresana C. Diversity of the enzymatic activity in the lipoxygenase gene family of Arabidopsis thaliana. Lipids. 2009; 44(2):85–95. https://doi.org/10.1007/s11745-008-3245-7 PMID: 18949503

105. Umate P. Genome-wide analysis of lipoxygenase gene family in Arabidopsis and rice. Plant Signal Behav. 2011; 6(3):335–8. https://doi.org/10.4161/psb.6.3.13546 PMID: 21336026

106. Chen Z, Chen D, Chu W, Zhu D, Yan H, Xiang Y. Retention and Molecular Evolution of Lipoxygenase Genes in Modern Rosid Plants. Front Genet. 2016; 7:176. https://doi.org/10.3389/fgene.2016.00176 PMID: 27746812

107. Wang J, Hu T, Wang W, Hu H, Wei Q, Wei X, et al. Bioinformatics Analysis of the Lipoxygenase Gene Family in Radish (Raphanus sativus) and Functional Characterization in Response to Abiotic and Biotic Stresses. Int J Mol Sci. 2019; 20(23):6095. https://doi.org/10.3390/ijms20236095 PMID: 31816887

108. Yan C, Jia K, Zhang J, Xiao Z, Sha X, Gao J, et al. Genome-wide identification and expression pattern analysis of lipoxygenase gene family in turnip (Brassica rapa L. subsp. rapa). PeerJ. 2022; 10:e13746. https://doi.org/10.7717/peerj.13746 PMID: 35898937

109. Yang XY, Jiang WJ, Yu HJ. The expression profiling of the lipoxygenase (LOX) family genes during fruit development, abiotic stress and hormonal treatments in cucumber (Cucumis sativus L.). Int J Mol Sci. 2012; 13(2):2481–500. https://doi.org/10.3390/ijms13022481 PMID: 22408466

110. Liu S, Liu X, Jiang L. Genome-wide identification, phylogeny and expression analysis of the lipoxygenase gene family in cucumber. Genet Mol Res. 2011; 10(4):2613–36. https://doi.org/10.4238/2011.October.25.9 PMID: 22057958

111. Zhang C, Jin YZ, Liu JY, Tang YF, Cao SX, Qi HY. The phylogeny and expression profiles of the lipoxygenase (LOX) family genes in the melon (Cucumis melo L.) genome. Scientia Horticulturae. 2014; 170:94–102.

112. Liu JP, Zhou Y, Li JW, Wang F, Yang YX. Comprehensive Genomic Characterization and Expression Analysis of the Lipoxygenase Gene Family in Watermelon under Hormonal Treatments. Agriculture-Basel. 2020; 10(10):429.

113. Mou Y, Sun Q, Yuan C, Zhao X, Wang J, Yan C, et al. Identification of the LOX Gene Family in Peanut and Functional Characterization of AhLOX29 in Drought Tolerance. Front Plant Sci. 2022; 13:832785. https://doi.org/10.3389/fpls.2022.832785 PMID: 35356112

114. Shin JH, Van K, Kim DH, Kim KD, Jang YE, Choi BS, et al. The lipoxygenase gene family: a genomic fossil of shared polyploidy between Glycine max and Medicago truncatula. BMC Plant Biol. 2008; 8 (1):133.

115. Shaban M, Ahmed MM, Sun H, Ullah A, Zhu L. Genome-wide identification of lipoxygenase gene family in cotton and functional characterization in response to abiotic stresses. BMC Genomics. 2018; 19 (1):599. https://doi.org/10.1186/s12864-018-4985-2 PMID: 30092779

116. Liu F, Li H, Wu J, Wang B, Tian N, Liu J, et al. Genome-wide identification and expression pattern analysis of lipoxygenase gene family in banana. Sci Rep. 2021; 11(1):9948. https://doi.org/10.1038/s41598-021-89211-6 PMID: 33976263

117. Ogunola OF, Hawkins LK, Mylroie E, Kolomiets MV, Borrego E, Tang JD, et al. Characterization of the maize lipoxygenase gene family in relation to aflatoxin accumulation resistance. PLoS One. 2017; 12 (7):e0181265. https://doi.org/10.1371/journal.pone.0181265 PMID: 28715485

118. Zhang Q, Zhao Y, Zhang J, Li X, Ma F, Duan M, et al. The Responses of the Lipoxygenase Gene Family to Salt and Drought Stress in Foxtail Millet (Setaria italica). Life (Basel). 2021; 11(11):1169. https://doi.org/10.3390/life11111169 PMID: 34833045

119. Shrestha K, Pant S, Huang Y. Genome-wide identification and classification of Lipoxygenase gene family and their roles in sorghum-aphid interaction. Plant Mol Biol. 2021; 105(4–5):527–41. https://doi.org/10.1007/s11103-020-01107-7 PMID: 33387173

120. Ji QQ, Zhang TY, Zhang D, Lv SM, Tan AJ. Genome-wide identification and expression analysis of lipoxygenase genes in Tartary buckwheat. Biotechnology & Biotechnological Equipment. 2020; 34 (1):273–86.

121. Li JD, Chen LC, Chen P, Li QC, Yang QQ, Zhang Y, et al. Genome-wide identification and expression of the lipoxygenase gene family in jujube (Ziziphus jujuba) in response to phytoplasma infection. Journal of Plant Biochemistry and Biotechnology. 2022; 31(1):139–53.

122. Vogt J, Schiller D, Ulrich D, Schwab W, Dunemann F. Identification of lipoxygenase (LOX) genes putatively involved in fruit flavour formation in apple (Malus x domestica). Tree Genetics & Genomes. 2013; 9(6):1493–511.

123. Guo SL, Song ZZ, Ma RJ, Yang Y, Yu ML. Genome-wide identification and expression analysis of the lipoxygenase gene family during peach fruit ripening under different postharvest treatments. Acta Physiologiae Plantarum. 2017; 39(5):111.

124. Li M, Li L, Dunwell JM, Qiao X, Liu X, Zhang S. Characterization of the lipoxygenase (LOX) gene family in the Chinese white pear (Pyrus bretschneideri) and comparison with other members of the Rosaceae. BMC Genomics. 2014; 15(1):444. https://doi.org/10.1186/1471-2164-15-444 PMID: 24906560

125. Chen Z, Chen X, Yan H, Li W, Li Y, Cai R, et al. The Lipoxygenase Gene Family in Poplar: Identification, Classification, and Expression in Response to MeJA Treatment. PLoS One. 2015; 10(4): e0125526. https://doi.org/10.1371/journal.pone.0125526 PMID: 25928711

126. Sarde SJ, Kumar A, Remme RN, Dicke M. Genome-wide identification, classification and expression of lipoxygenase gene family in pepper. Plant Mol Biol. 2018; 98(4–5):375–87. https://doi.org/10.1007/s11103-018-0785-y PMID: 30317456

127. Upadhyay RK, Handa AK, Mattoo AK. Transcript Abundance Patterns of 9- and 13-Lipoxygenase Subfamily Gene Members in Response to Abiotic Stresses (Heat, Cold, Drought or Salt) in Tomato (Solanum lycopersicum L.) Highlights Member-Specific Dynamics Relevant to Each Stress. Genes (Basel). 2019; 10(9):683. https://doi.org/10.3390/genes10090683 PMID: 31492025

128. Upadhyay RK, Mattoo AK. Genome-wide identification of tomato (Solanum lycopersicum L.) lipoxygenases coupled with expression profiles during plant development and in response to methyl-jasmonate and wounding. J Plant Physiol. 2018; 231:318–28. https://doi.org/10.1016/j.jplph.2018.10.001 PMID: 30368230

129. Zhu J, Wang X, Guo L, Xu Q, Zhao S, Li F, et al. Characterization and Alternative Splicing Profiles of the Lipoxygenase Gene Family in Tea Plant (Camellia sinensis). Plant Cell Physiol. 2018; 59(9):1765–81. https://doi.org/10.1093/pcp/pcy091 PMID: 29726968

130. Podolyan A, White J, Jordan B, Winefield C. Identification of the lipoxygenase gene family from Vitis vinifera and biochemical characterisation of two 13-lipoxygenases expressed in grape berries of Sauvignon Blanc. Functional Plant Biology. 2010; 37(8):767–84.

131. Mochizuki S, Sugimoto K, Koeduka T, Matsui K. Arabidopsis lipoxygenase 2 is essential for formation of green leaf volatiles and five-carbon volatiles. FEBS letters. 2016; 590(7):1017–27. https://doi.org/10.1002/1873-3468.12133 PMID: 26991128

132. Conneely LJ, Mauleon R, Mieog J, Barkla BJ, Kretzschmar T. Characterization of the Cannabis sativa glandular trichome proteome. PLoS One. 2021; 16(4):e0242633. https://doi.org/10.1371/journal.pone.0242633 PMID: 33793557

133. Watts S, McElroy M, Migicovsky Z, Maassen H, van Velzen R, Myles S. Cannabis labelling is associated with genetic variation in terpene synthase genes. Nat Plants. 2021; 7(10):1330–4. https://doi.org/10.1038/s41477-021-01003-y PMID: 34650264

134. Rice S, Koziel JA. Characterizing the Smell of Marijuana by Odor Impact of Volatile Compounds: An Application of Simultaneous Chemical and Sensory Analysis. PLoS One. 2015; 10(12):e0144160. https://doi.org/10.1371/journal.pone.0144160 PMID: 26657499

135. Zhou Y, Guang YL, Li JW, Wang F, Ahammed GJ, Yang YX. The CYP74 Gene Family in Watermelon: Genome-Wide Identification and Expression Profiling Under Hormonal Stress and Root-Knot Nematode Infection. Agronomy-Basel. 2019; 9(12):872.

136. De Domenico S, Taurino M, Gallo A, Poltronieri P, Pastor V, Flors V, et al. Oxylipin dynamics in Medicago truncatula in response to salt and wounding stresses. Physiol Plant. 2019; 165(2):198–208. https://doi.org/10.1111/ppl.12810 PMID: 30051613

137. Xiong R, He T, Wang Y, Liu S, Gao Y, Yan H, et al. Genome and transcriptome analysis to understand the role diversification of cytochrome P450 gene under excess nitrogen treatment. BMC Plant Biol. 2021; 21(1):447. https://doi.org/10.1186/s12870-021-03224-x PMID: 34615481

138. Froehlich JE, Itoh A, Howe GA. Tomato allene oxide synthase and fatty acid hydroperoxide lyase, two cytochrome P450s involved in oxylipin metabolism, are targeted to different membranes of chloroplast envelope. Plant Physiol. 2001; 125(1):306–17. https://doi.org/10.1104/pp.125.1.306 PMID: 11154338

139. Toporkova YY, Askarova EK, Gorina SS, Ogorodnikova AV, Mukhtarova LS, Grechkin AN. Epoxyalcohol synthase activity of the CYP74B enzymes of higher plants. Biochim Biophys Acta Mol Cell Biol Lipids. 2020; 1865(9):158743. https://doi.org/10.1016/j.bbalip.2020.158743 PMID: 32464332

140. Toporkova YY, Gogolev YV, Mukhtarova LS, Grechkin AN. Determinants governing the CYP74 catalysis: conversion of allene oxide synthase into hydroperoxide lyase by site-directed mutagenesis. FEBS Lett. 2008; 582(23–24):3423–8. https://doi.org/10.1016/j.febslet.2008.09.005 PMID: 18789329

141. Lee DS, Nioche P, Hamberg M, Raman CS. Structural insights into the evolutionary paths of oxylipin biosynthetic enzymes. Nature. 2008; 455(7211):363–8. https://doi.org/10.1038/nature07307 PMID: 18716621

142. Wu Q, Wu J, Sun H, Zhang D, Yu D. Sequence and expression divergence of the AOC gene family in soybean: insights into functional diversity for stress responses. Biotechnol Lett. 2011; 33(7):1351–9. https://doi.org/10.1007/s10529-011-0585-9 PMID: 21626009

143. Stenzel I, Otto M, Delker C, Kirmse N, Schmidt D, Miersch O, et al. ALLENE OXIDE CYCLASE (AOC) gene family members of Arabidopsis thaliana: tissue- and organ-specific promoter activities and in vivo heteromerization. J Exp Bot. 2012; 63(17):6125–38. https://doi.org/10.1093/jxb/ers261 PMID: 23028017

144. Otto M, Naumann C, Brandt W, Wasternack C, Hause B. Activity Regulation by Heteromerization of Arabidopsis Allene Oxide Cyclase Family Members. Plants (Basel). 2016; 5(1):3. https://doi.org/10.3390/plants5010003 PMID: 27135223

145. Matsui H, Nakamura G, Ishiga Y, Toshima H, Inagaki Y, Toyoda K, et al. Structure and expression of 12-oxophytodienoate reductase (subgroup I) genes in pea, and characterization of the oxidoreductase activities of their recombinant products. Mol Genet Genomics. 2004; 271(1):1–10. https://doi.org/10.1007/s00438-003-0948-6 PMID: 14727182

146. Guang Y, Luo S, Ahammed GJ, Xiao X, Li J, Zhou Y, et al. The OPR gene family in watermelon: Genome-wide identification and expression profiling under hormone treatments and root-knot nematode infection. Plant Biol (Stuttg). 2021; 23 Suppl 1:80–8.

147. Zhang J, Simmons C, Yalpani N, Crane V, Wilkinson H, Kolomiets M. Genomic analysis of the 12-oxophytodienoic acid reductase gene family of Zea mays. Plant Mol Biol. 2005; 59(2):323–43. https://doi.org/10.1007/s11103-005-8883-z PMID: 16247560

148. Liu S, Sun R, Zhang X, Feng Z, Wei F, Zhao L, et al. Genome-Wide Analysis of OPR Family Genes in Cotton Identified a Role for GhOPR9 in Verticillium dahliae Resistance. Genes (Basel). 2020; 11(10):1134. https://doi.org/10.3390/genes11101134 PMID: 32992523

149. Li W, Zhou F, Liu B, Feng D, He Y, Qi K, et al. Comparative characterization, expression pattern and function analysis of the 12-oxo-phytodienoic acid reductase gene family in rice. Plant Cell Rep. 2011; 30(6):981–95. https://doi.org/10.1007/s00299-011-1002-5 PMID: 21249367

150. Mou Y, Liu Y, Tian S, Guo Q, Wang C, Wen S. Genome-Wide Identification and Characterization of the OPR Gene Family in Wheat (Triticum aestivum L.). Int J Mol Sci. 2019; 20(8):1914. https://doi.org/10.3390/ijms20081914 PMID: 31003470

151. Sobajima H, Takeda M, Sugimori M, Kobashi N, Kiribuchi K, Cho EM, et al. Cloning and characterization of a jasmonic acid-responsive gene encoding 12-oxophytodienoic acid reductase in suspension-cultured rice cells. Planta. 2003; 216(4):692–8. https://doi.org/10.1007/s00425-002-0909-z PMID: 12569412

152. Farmer EE, Davoine C. Reactive electrophile species. Curr Opin Plant Biol. 2007; 10(4):380–6. https://doi.org/10.1016/j.pbi.2007.04.019 PMID: 17646124

153. Li W, Liu B, Yu L, Feng D, Wang H, Wang J. Phylogenetic analysis, structural evolution and functional divergence of the 12-oxo-phytodienoate acid reductase gene family in plants. BMC Evol Biol. 2009; 9 (1):90. https://doi.org/10.1186/1471-2148-9-90 PMID: 19416520

154. Apicella PV, Sands LB, Ma Y, Berkowitz GA. Delineating genetic regulation of cannabinoid biosynthesis during female flower development in Cannabis sativa. Plant Direct. 2022; 6(6):e412. https://doi.org/10.1002/pld3.412 PMID: 35774623

155. Garrido J, Rico S, Corral C, Sánchez C, Vidal N, Martínez-Quesada JJ, et al. Exogenous application of stress-related signaling molecules affect growth and cannabinoid accumulation in medical cannabis (Cannabis sativa L.). Frontiers in Plant Science. 2022; 13:5219. https://doi.org/10.3389/fpls.2022.1082554 PMID: 36605951

156. Flores-Sanchez IJ, Peč J, Fei J, Choi YH, Dušek J, Verpoorte R. Elicitation studies in cell suspension cultures of Cannabis sativa L. Journal of biotechnology. 2009; 143(2):157–68. https://doi.org/10.1016/j.jbiotec.2009.05.006 PMID: 19500620

157. Kumeroa F, Komahan S, Sofkova-Bobcheva S, Clavijo McCormick A. Characterization of the Volatile Profiles of Six Industrial Hemp (Cannabis sativa L.) Cultivars. Agronomy. 2022; 12(11):2651.

158. Song W, Yin H, Zhong Y, Wang D, Xu W, Deng Y. Regional differentiation based on volatile compounds via HS-SPME/GC–MS and chemical compositions comparison of hemp (Cannabis sativa L.) seeds. Food Research International. 2022; 162:112151. https://doi.org/10.1016/j.foodres.2022.112151 PMID: 36461412

159. Pavlovic R, Nenna G, Calvi L, Panseri S, Borgonovo G, Giupponi L, et al. Quality traits of "cannabidiol oils": cannabinoids content, terpene fingerprint and oxidation stability of European commercially available preparations. Molecules. 2018; 23(5):1230. https://doi.org/10.3390/molecules23051230 PMID: 29783790

160. Tura M, Ansorena D, Astiasarán I, Mandrioli M, Toschi TG. Evaluation of hemp seed oils stability under accelerated storage test. Antioxidants. 2022; 11(3):490. https://doi.org/10.3390/antiox11030490 PMID: 35326140

161. Welling MT, Deseo MA, Bacic A, Doblin MS. Untargeted metabolomic analyses reveal chemical complexity of dioecious cannabis flowers. Australian Journal of Chemistry. 2021; 74(6):463–79.

162. Balcke GU, Bennewitz S, Bergau N, Athmer B, Henning A, Majovsky P, et al. Multi-Omics of Tomato Glandular Trichomes Reveals Distinct Features of Central Carbon Metabolism Supporting High Productivity of Specialized Metabolites. Plant Cell. 2017; 29(5):960–83. https://doi.org/10.1105/tpc.17.00060 PMID: 28408661

163. Crombie WM. Fatty Acids in Chloroplasts and Leaves. Journal of Experimental Botany. 1958; 9 (26):254–61.

164. Poincelot RP. Lipid and Fatty Acid composition of chloroplast envelope membranes from species with differing net photosynthesis. Plant Physiol. 1976; 58(4):595–8. https://doi.org/10.1104/pp.58.4.595 PMID: 16659725

165. Engelberth J, Engelberth M. Variability in the Capacity to Produce Damage-Induced Aldehyde Green Leaf Volatiles among Different Plant Species Provides Novel Insights into Biosynthetic Diversity. Plants (Basel). 2020; 9(2):213. https://doi.org/10.3390/plants9020213 PMID: 32041302

166. Mano J, Belles-Boix E, Babiychuk E, Inze D, Torii Y, Hiraoka E, et al. Protection against photooxidative injury of tobacco leaves by 2-alkenal reductase. Detoxication of lipid peroxide-derived reactive carbonyls. Plant Physiol. 2005; 139(4):1773–83. https://doi.org/10.1104/pp.105.070391 PMID: 16299173

167. Maynard D, Kumar V, Sproß J, Dietz K-J. 12-oxophytodienoic acid reductase 3 (OPR3) functions as NADPH-dependent α, β-ketoalkene reductase in detoxification and monodehydroascorbate reductase in redox homeostasis. Plant and Cell Physiology. 2020; 61(3):584–95.

168. Tola AJ, Jaballi A, Germain H, Missihoun TD. Recent Development on Plant Aldehyde Dehydrogenase Enzymes and Their Functions in Plant Development and Stress Signaling. Genes (Basel). 2020; 12(1):51. https://doi.org/10.3390/genes12010051 PMID: 33396326

169. Li S, Hu PC, Malmstadt N. Imaging molecular transport across lipid bilayers. Biophys J. 2011; 101 (3):700–8. https://doi.org/10.1016/j.bpj.2011.06.044 PMID: 21806938

170. Zhang C, Cao S, Jin Y, Ju L, Chen Q, Xing Q, et al. Melon13-lipoxygenase CmLOX18 may be involved in C6 volatiles biosynthesis in fruit. Scientific Reports. 2017; 7(1):2816. https://doi.org/10.1038/s41598-017-02559-6 PMID: 28588227

171. Piovesana S, Aita SE, Cannazza G, Capriotti AL, Cavaliere C, Cerrato A, et al. In-depth cannabis fatty acid profiling by ultra-high performance liquid chromatography coupled to high resolution mass spectrometry. Talanta. 2021; 228:122249. https://doi.org/10.1016/j.talanta.2021.122249 PMID: 33773747

172. Pathi KM, Rink P, Budhagatapalli N, Betz R, Saado I, Hiekel S, et al. Engineering Smut Resistance in Maize by Site-Directed Mutagenesis of LIPOXYGENASE 3. Front Plant Sci. 2020; 11:543895. https://doi.org/10.3389/fpls.2020.543895 PMID: 33193477

173. Abbaraju HKR, Gupta R, Appenzeller LM, Fallis LP, Hazebroek J, Zhu G, et al. A vegetative storage protein improves drought tolerance in maize. Plant Biotechnol J. 2022; 20(2):374–89. https://doi.org/10.1111/pbi.13720 PMID: 34614273

174. Wang J, Kuang HQ, Zhang ZH, Yang YQ, Yan L, Zhang MC, et al. Generation of seed lipoxygenase-free soybean using CRISPR-Cas9. Crop Journal. 2020; 8(3):432–9.